The Planetary Theory of Solar Activity Variability
A Review

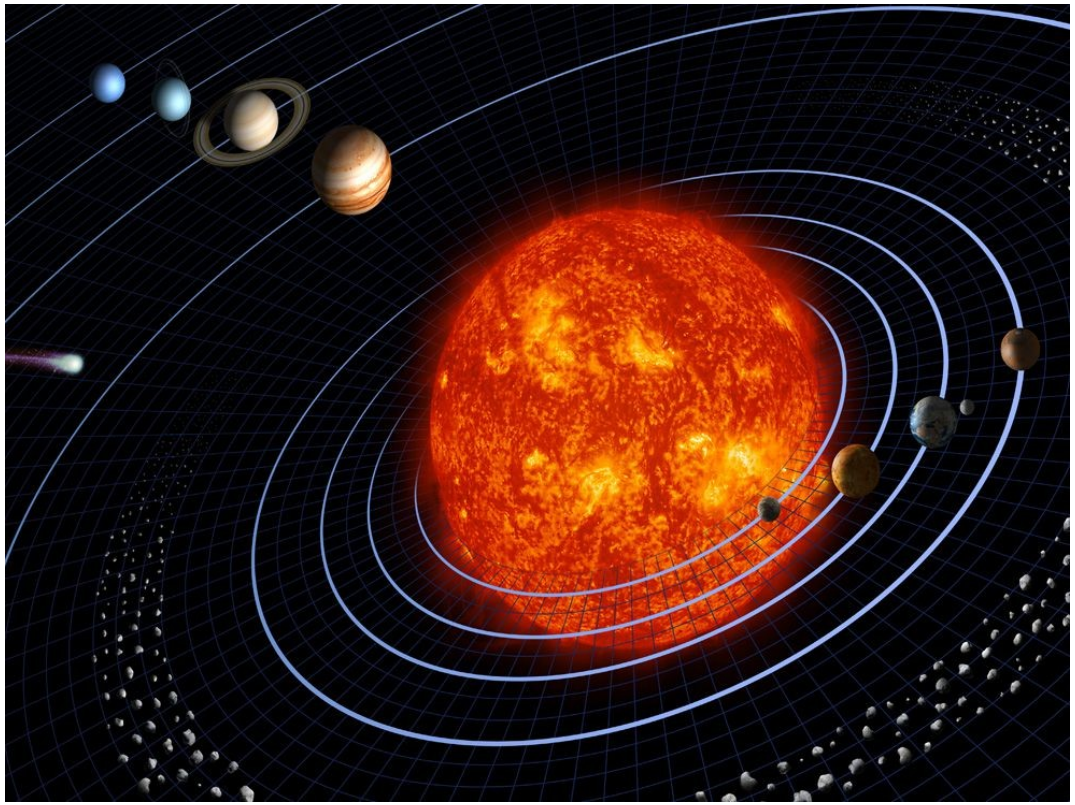

Scafetta N and Bianchini A (2022):
The Planetary Theory of Solar Activity Variability: A Review.
Front. Astron. Space Sci. 9:937930.
doi: 10.3389/fspas.2022.937930

Prof. Nicola Scafetta

26 November 2022

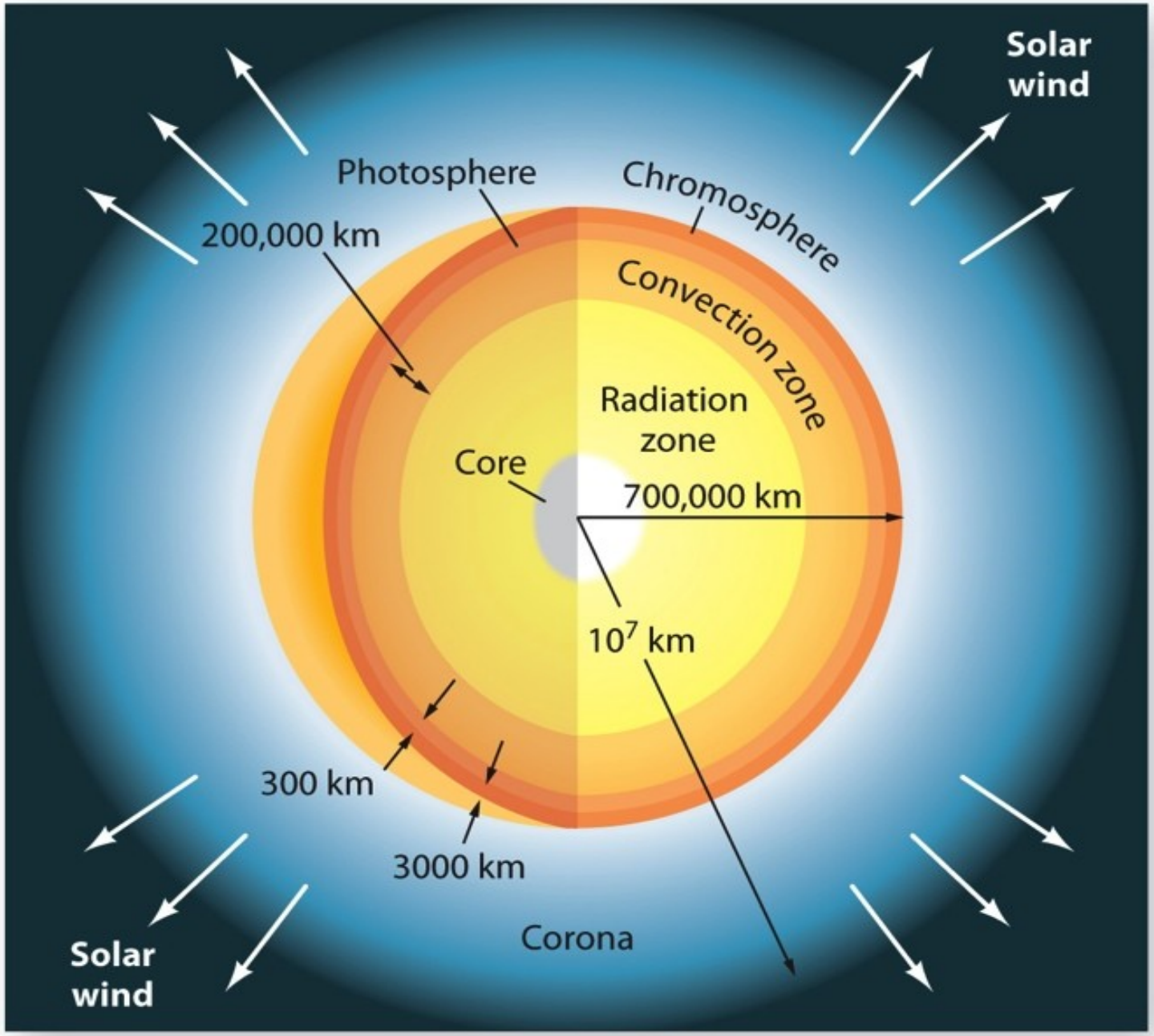

The Sun

- Source of all radiant energy
- 15 million degrees Kelvin at core
- Visible surface ~6,000 degrees Kelvin
- Magnetic fields create solar flares
- Total solar irradiance ~1,361 Wm^{-2}

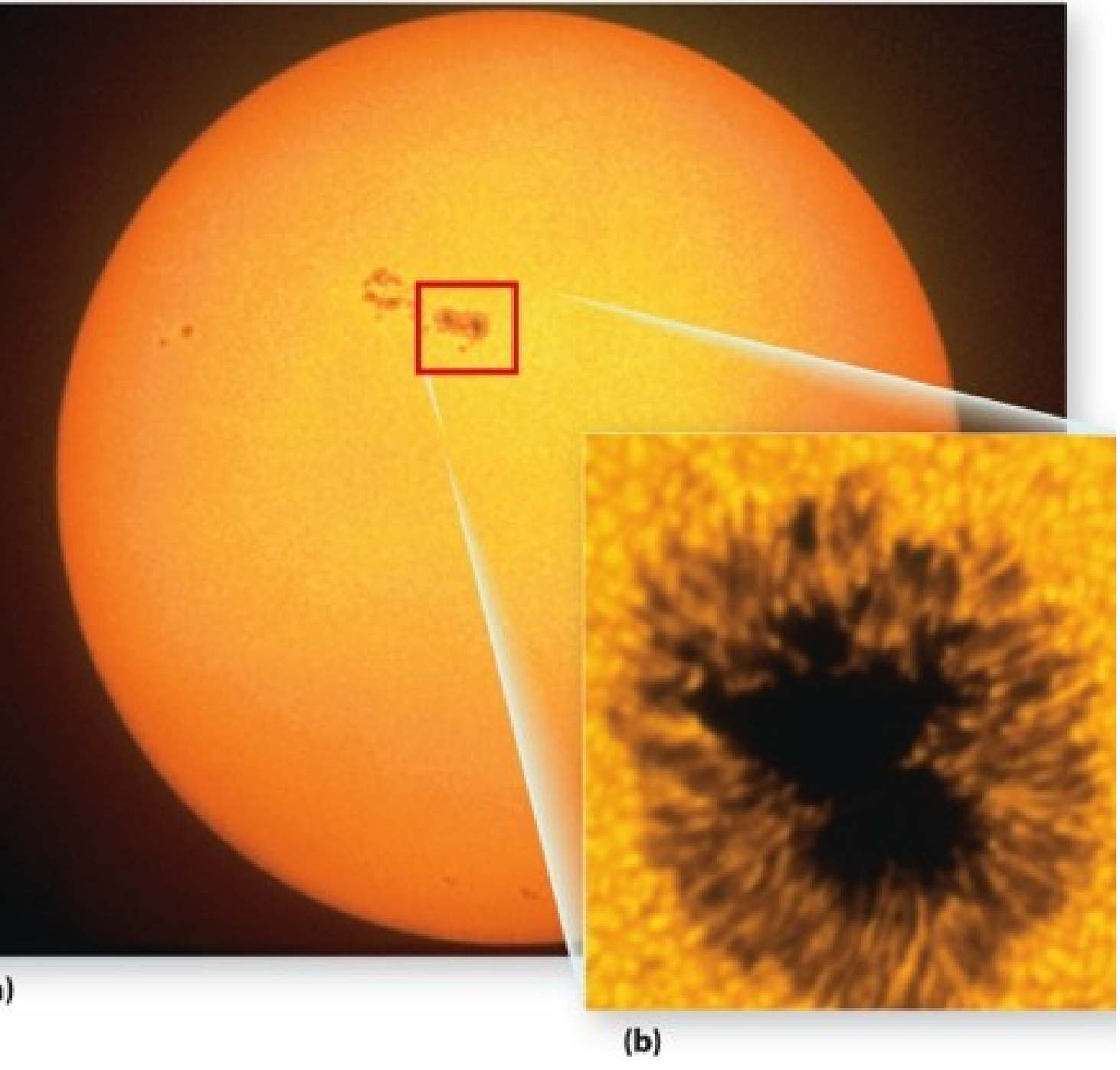

The Sun

- Sunspots:
  - Produced by magnetic fields
  - Cooler areas of the photosphere
  - Surrounded by brighter areas (faculae)
  - Rhythmic cycle called the Schwabe cycle
  - 11-year cycle most obvious
  - Other 22-, 45-, 60-, 85-, 100-150, 200-250, 500-, 1000-, 2,300-, and 6,000- year cycles

Sunspot activity and $\delta^{14}C$

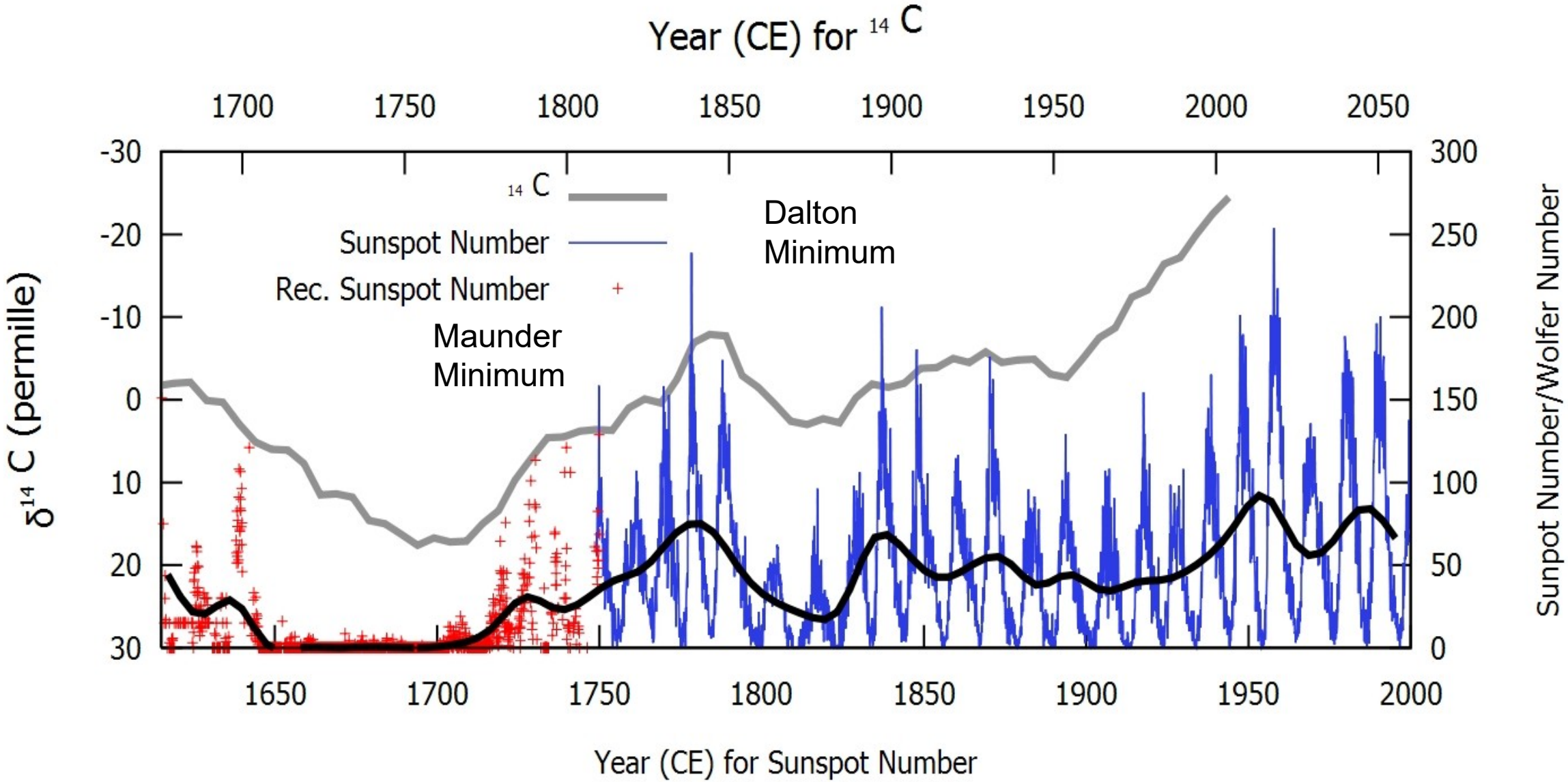

- Only solar activity has a millennial cycle.
- Which correlates with the millennial cycle of temperatures

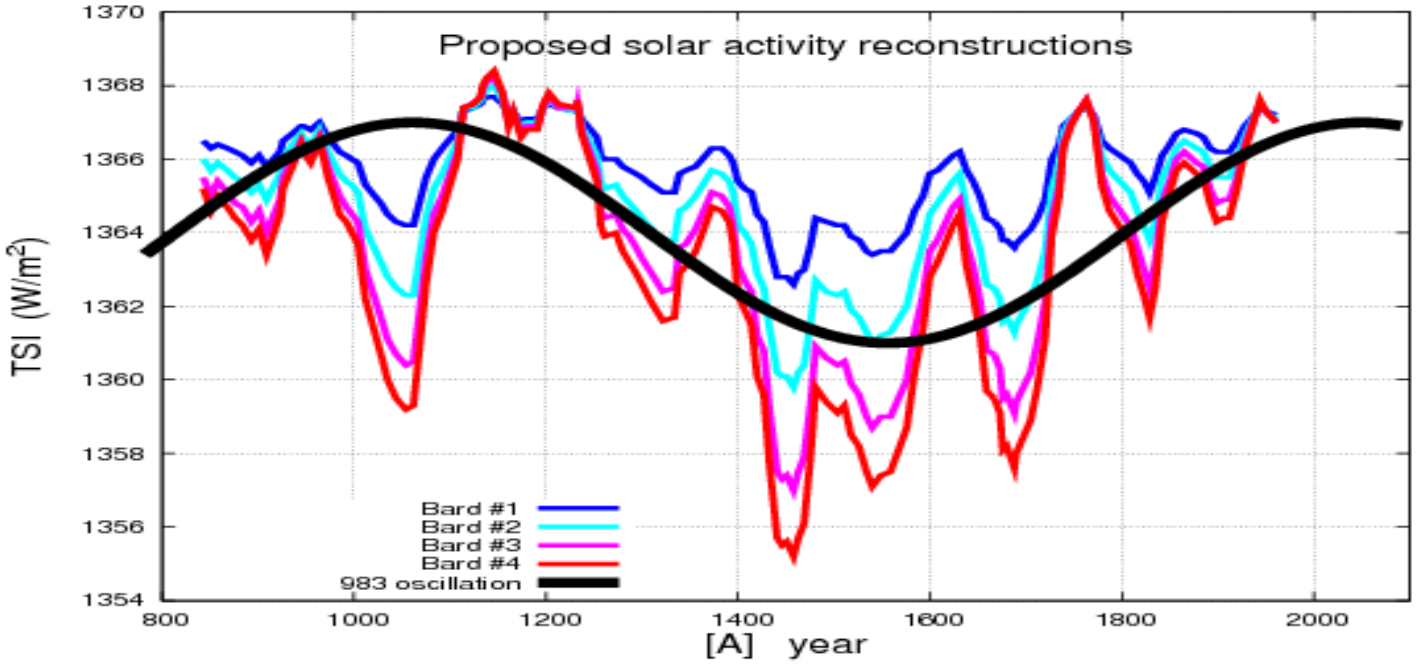

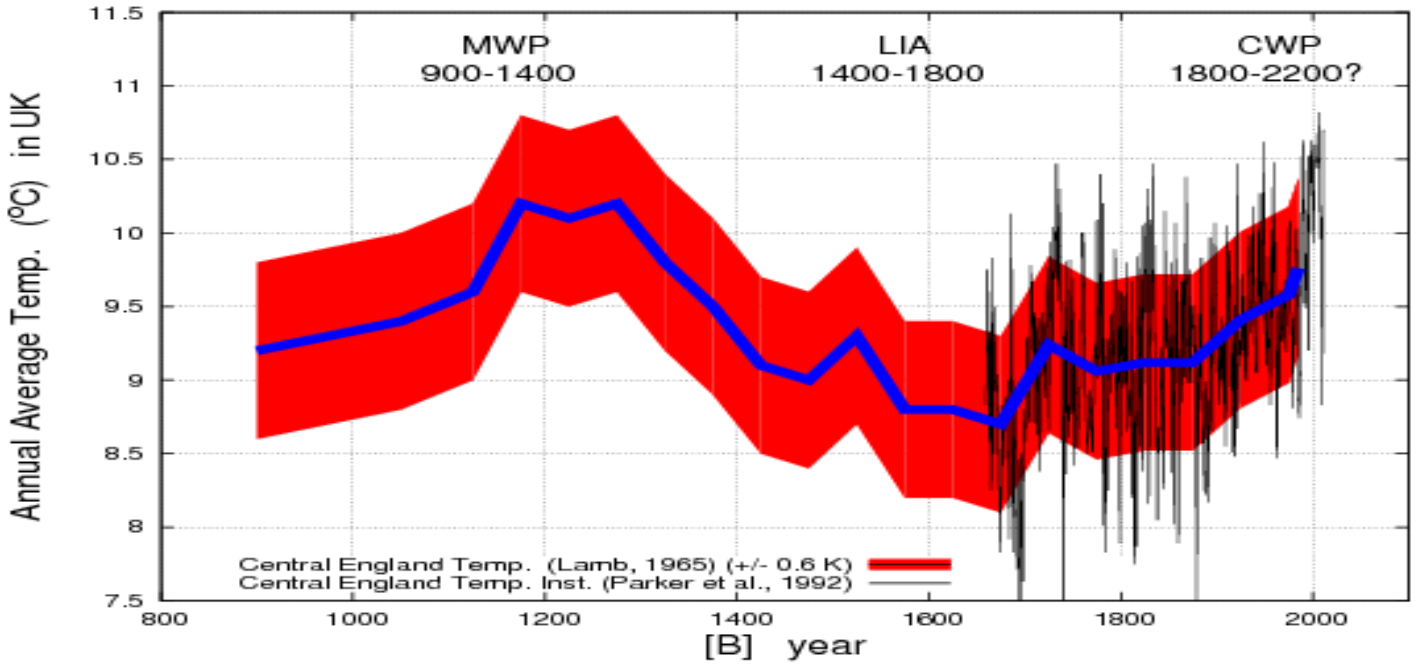

Central England Temperature

Holocene temperature vs. solar records

Comparison of solar activity (total solar irradiance [TSI]) in blue and $\delta^{18}O$ from Dongge cave, China, in green representing changes of the Asian climate. Possibly the Asian monsoon (AM) (low $\delta^{18}O$ corresponds to strong AM monsoon and vice versa).

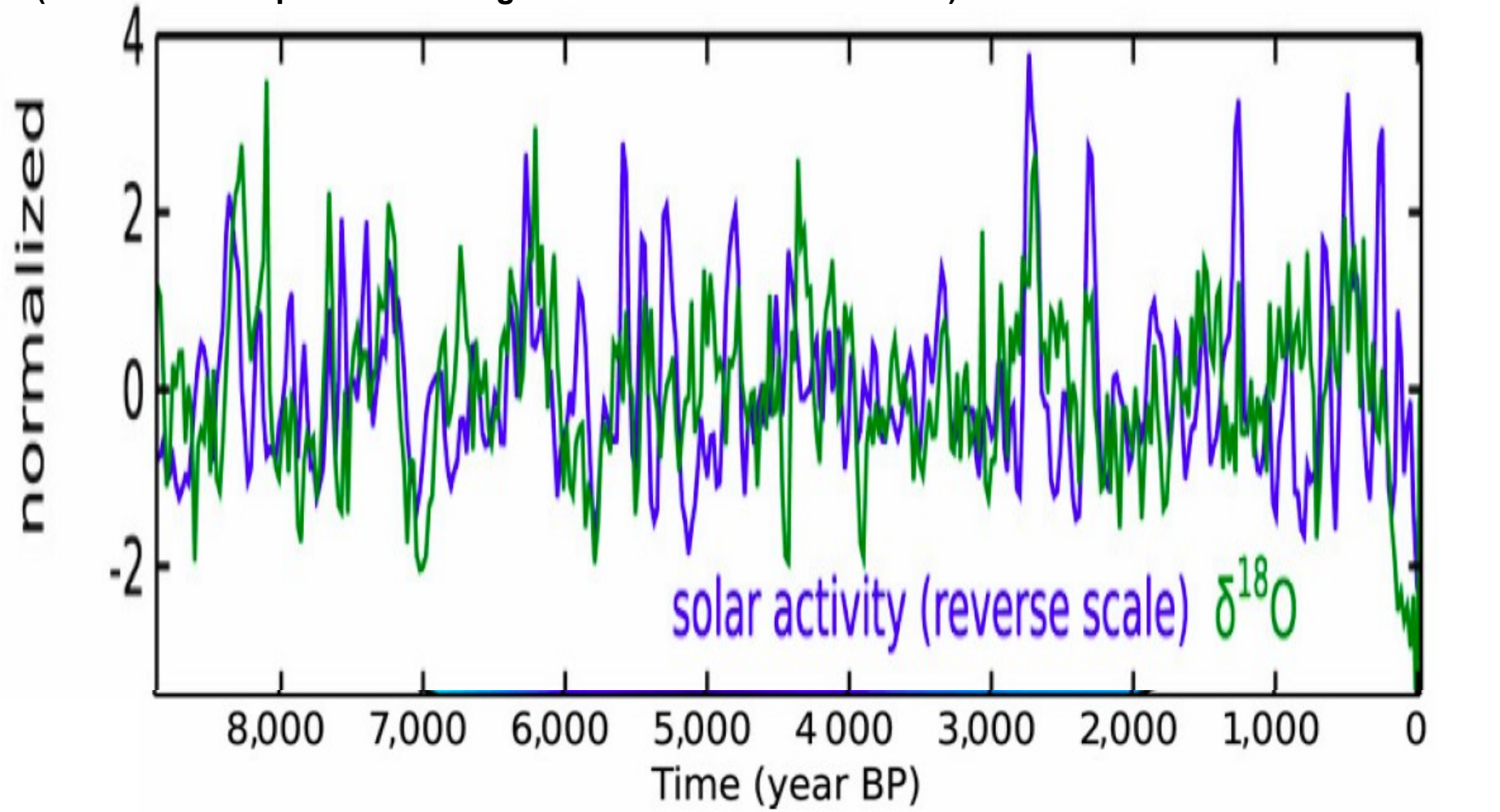

Steinhilber F et al. PNAS 2012;109:5967-5971

Total Solar Irradiance Records

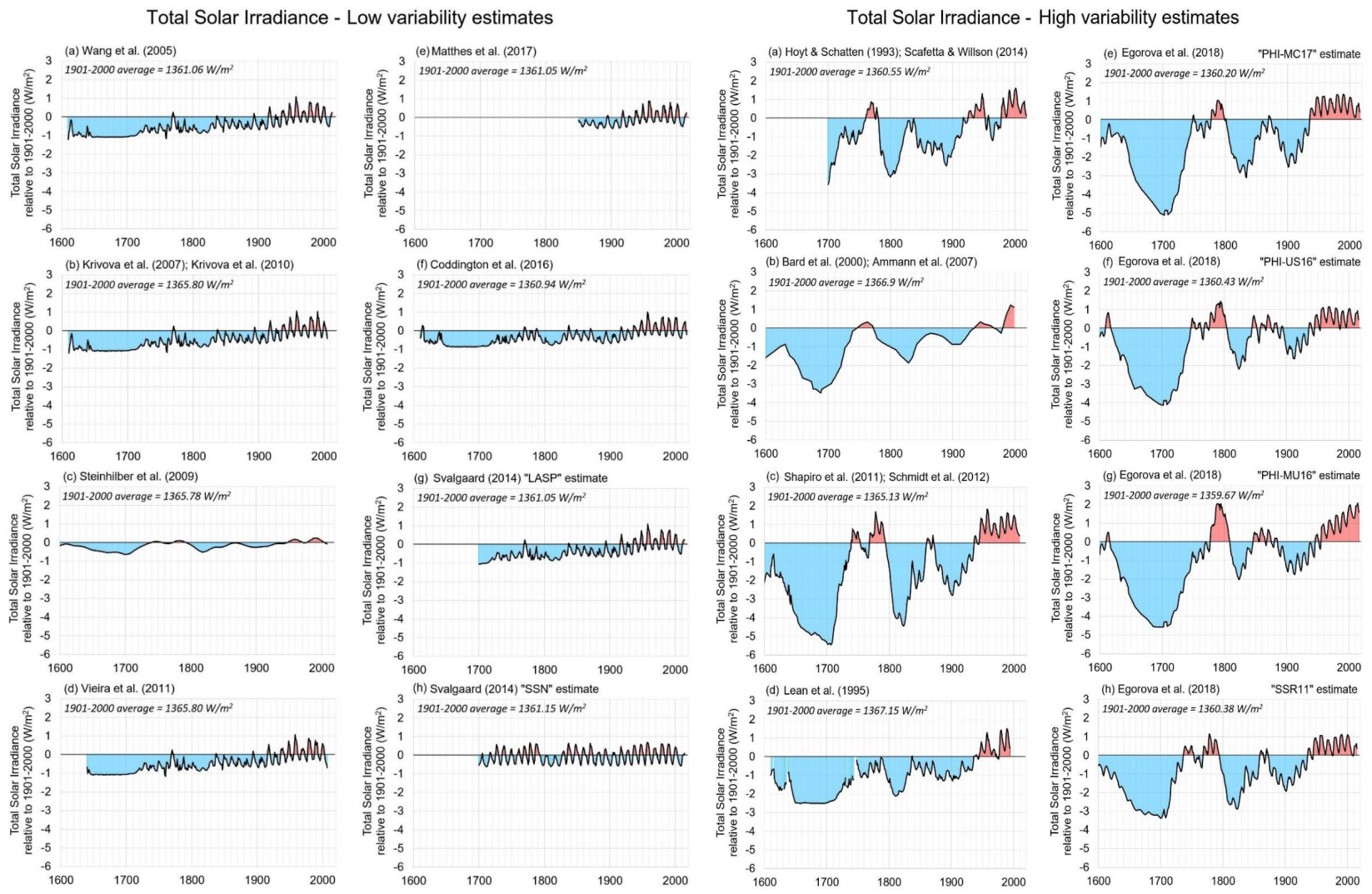

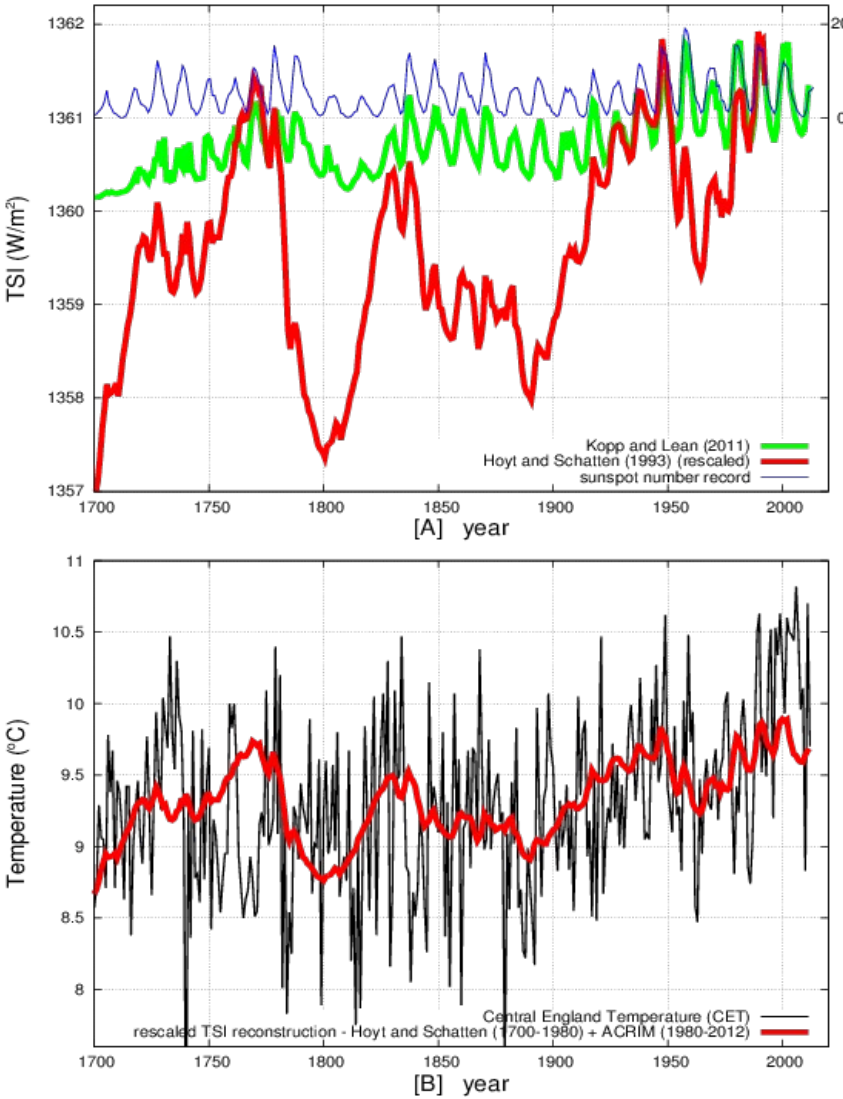

Connolly et al. How much has the Sun influenced Northern Hemisphere temperature trends? An ongoing debate. Research in Astronomy and Astrophysics (2021).

Uncertainty about solar reconstructions, and information on other sun-like stars

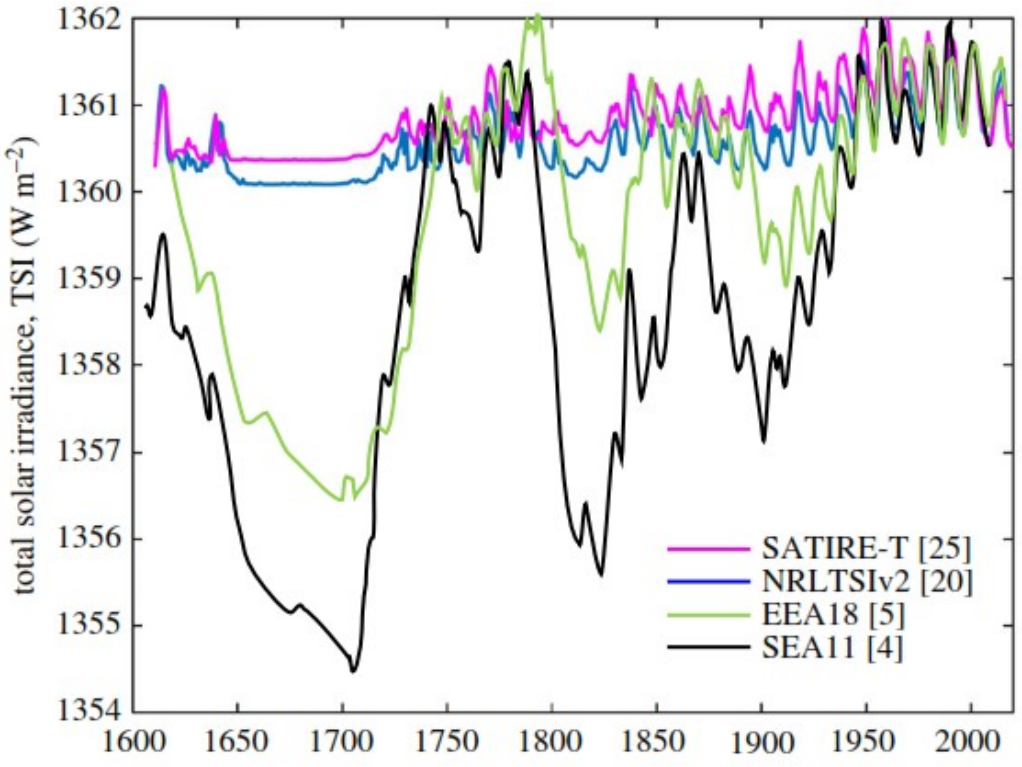

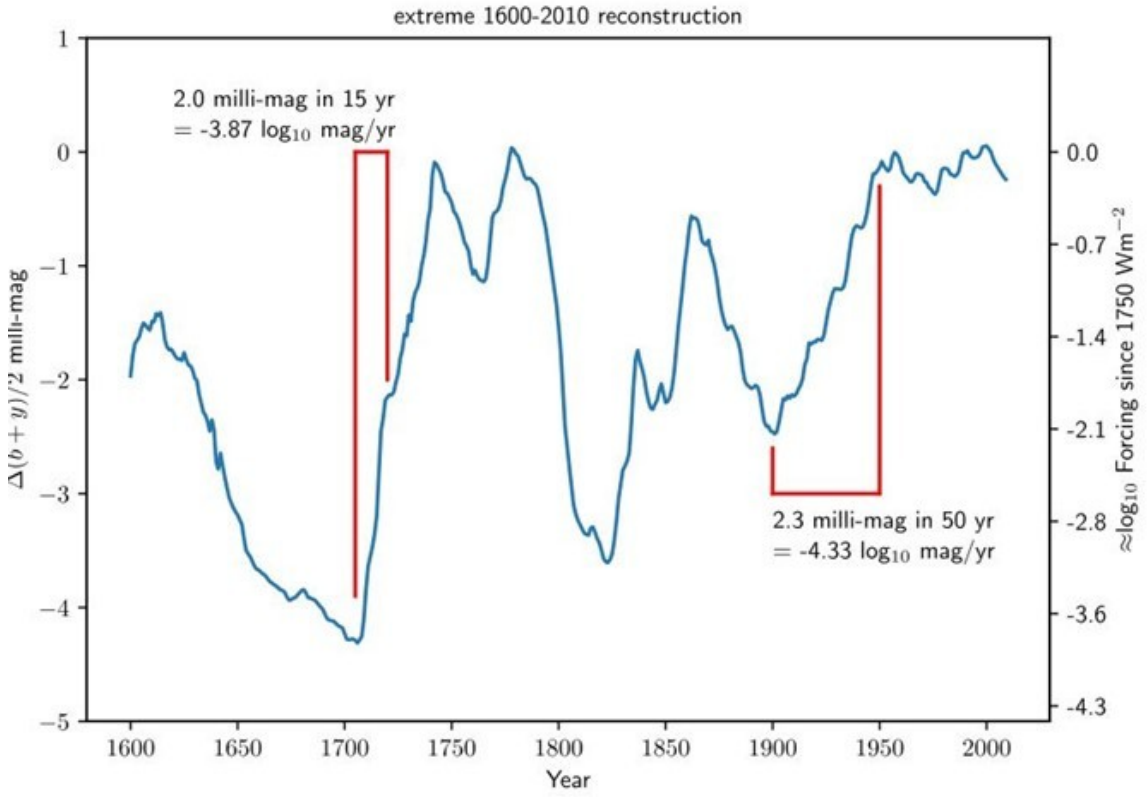

Uncertainty about the satellite solar reconstructions

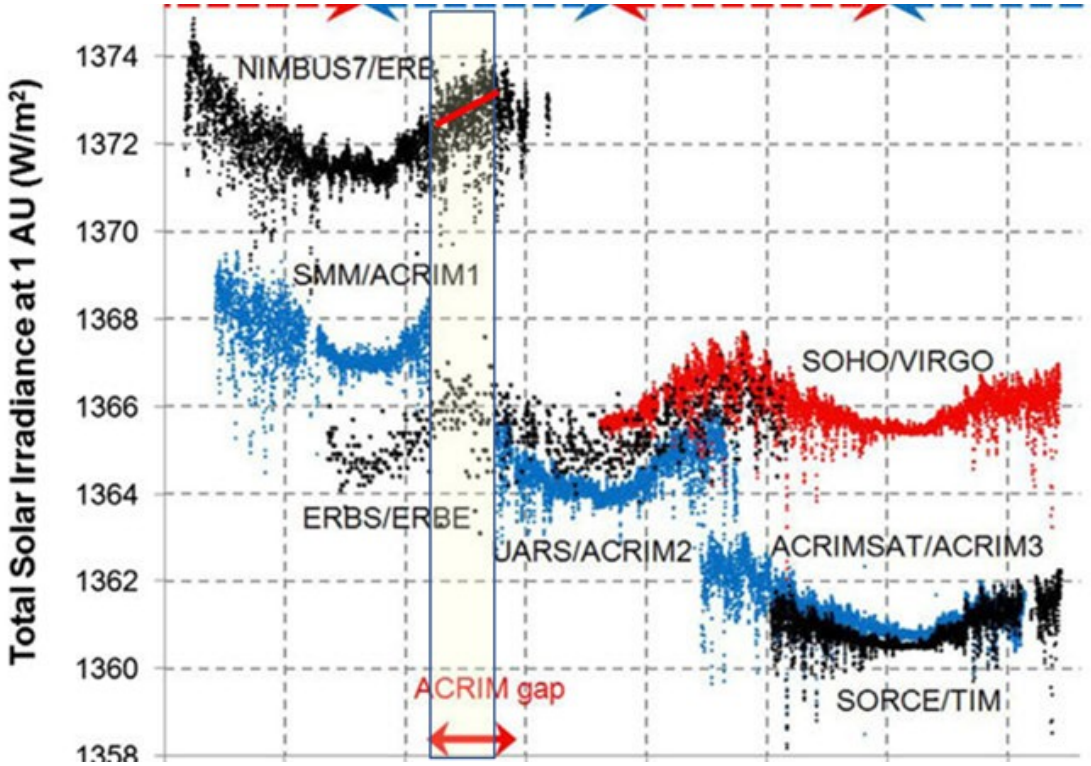

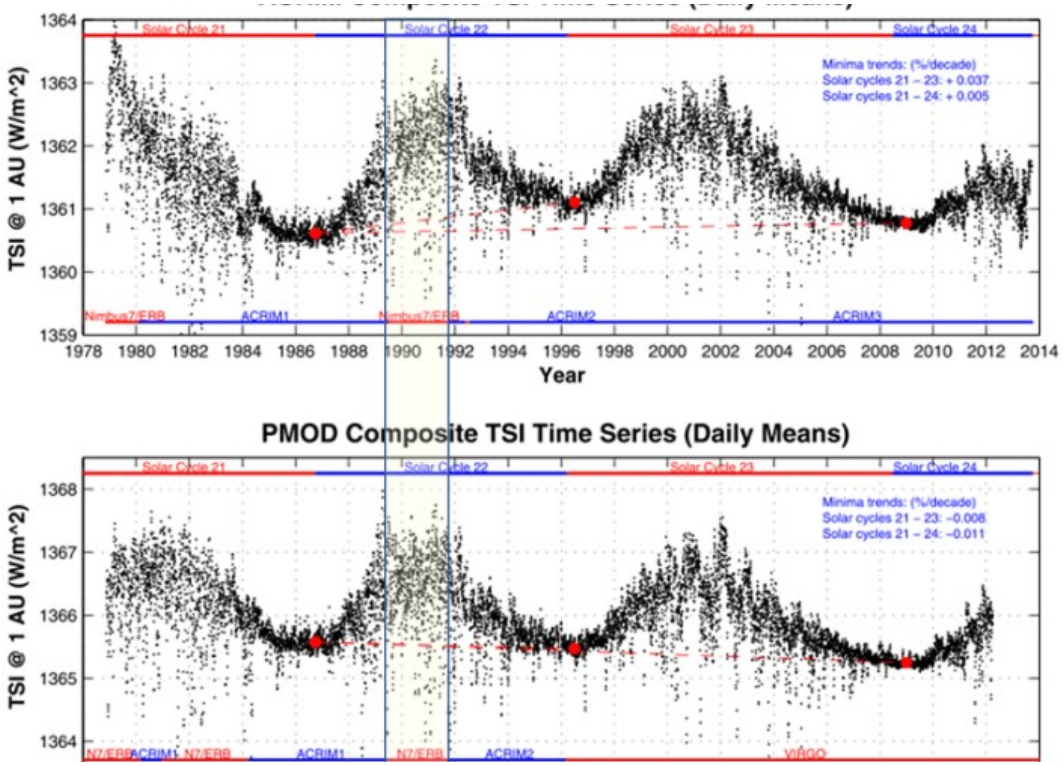

Different climate conclusions from different solar records

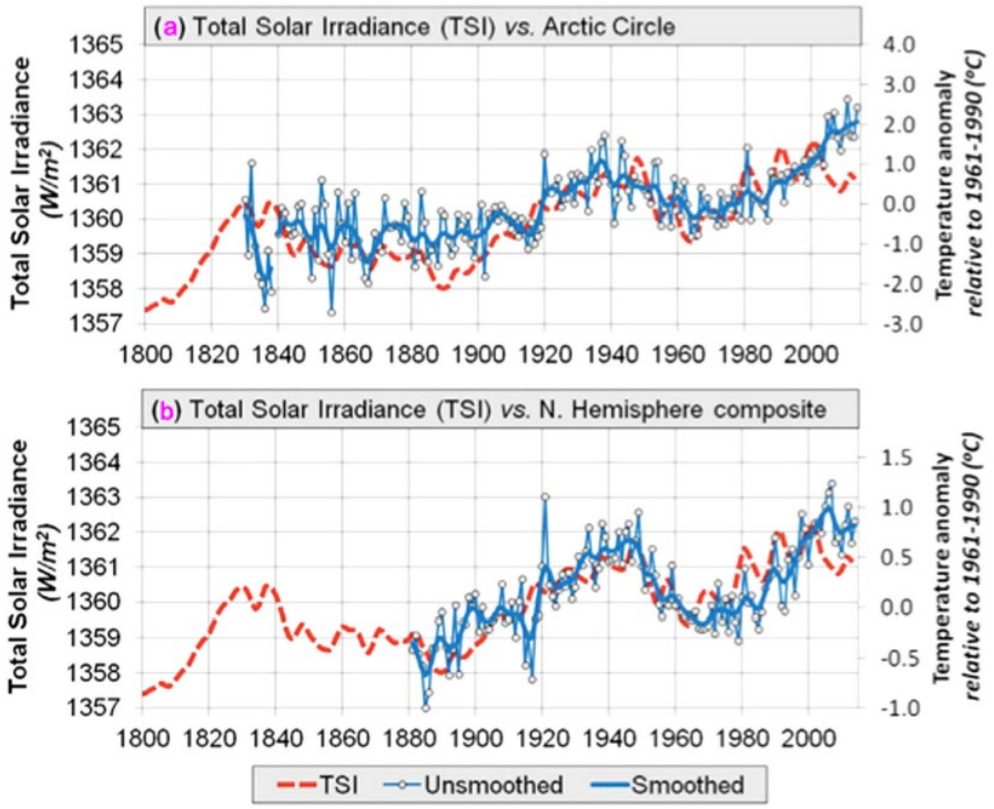

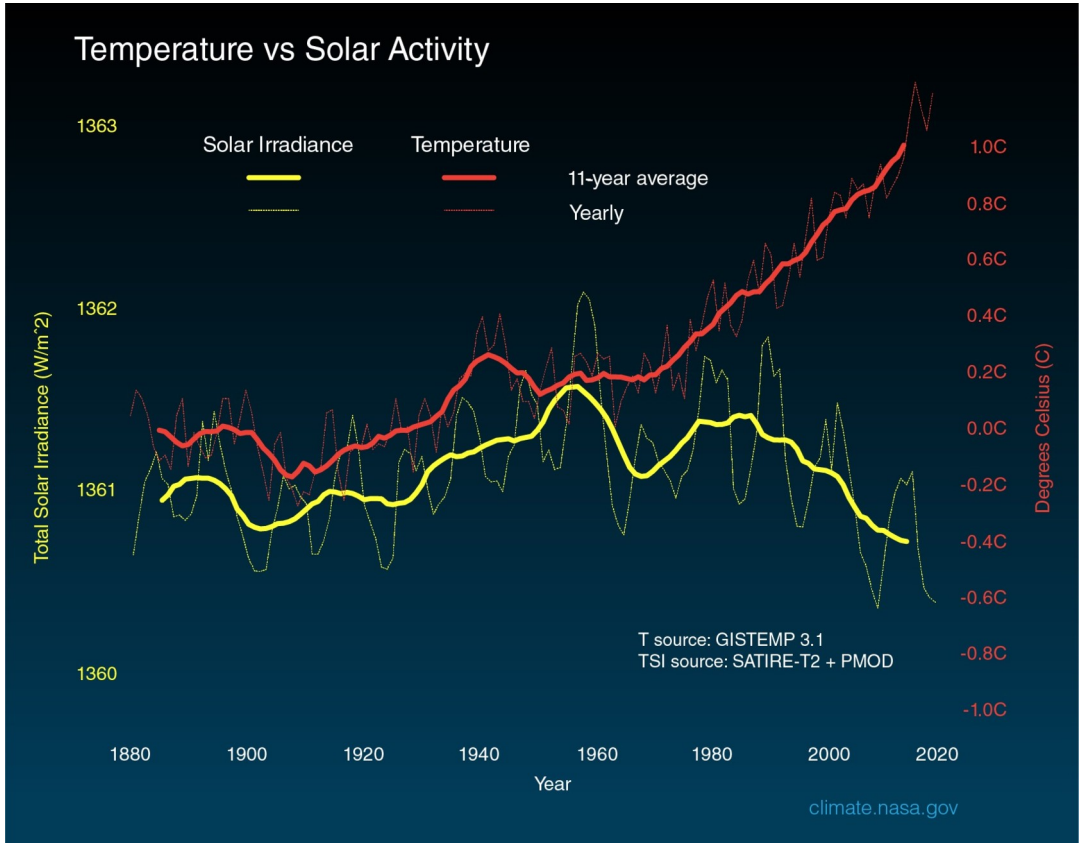

The Solar Dynamo: The Physical Basis of the Solar Cycle and the Sun's Magnetic Field

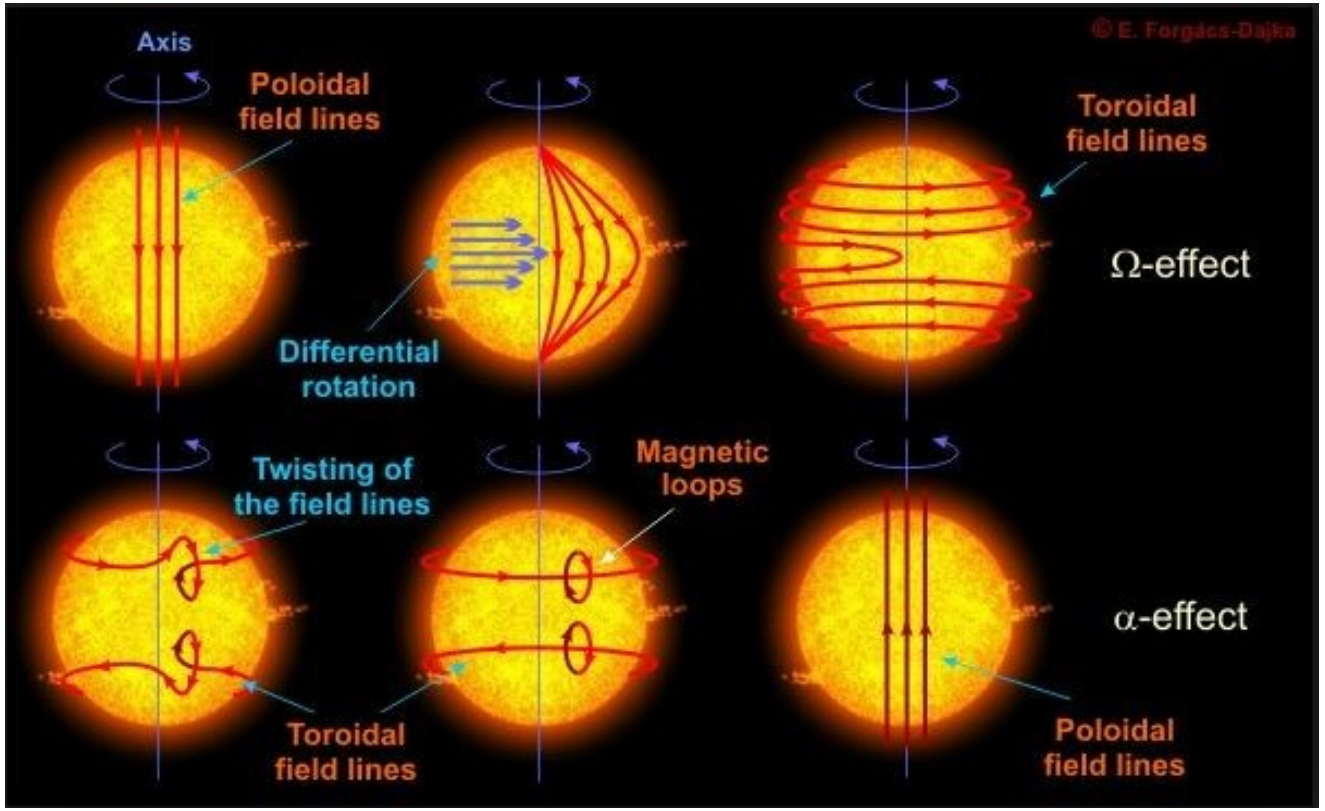

From a physical point of view, there are only two options: either solar activity changes are controlled solely by internal dynamo mechanisms, or the solar dynamo itself is partially synchronized by external harmonic planetary forcings, e.g. tides or other possible mechanisms.

Harmonics in solar records

- Ogurtsov, M.G., Nagovitsyn, Y.A., Kocharov, G.E., Jungner, H., 2002. Long-period cycles of the sun's activity recorded in direct solar data and proxies. Sol. Phys. 211, 371–394.

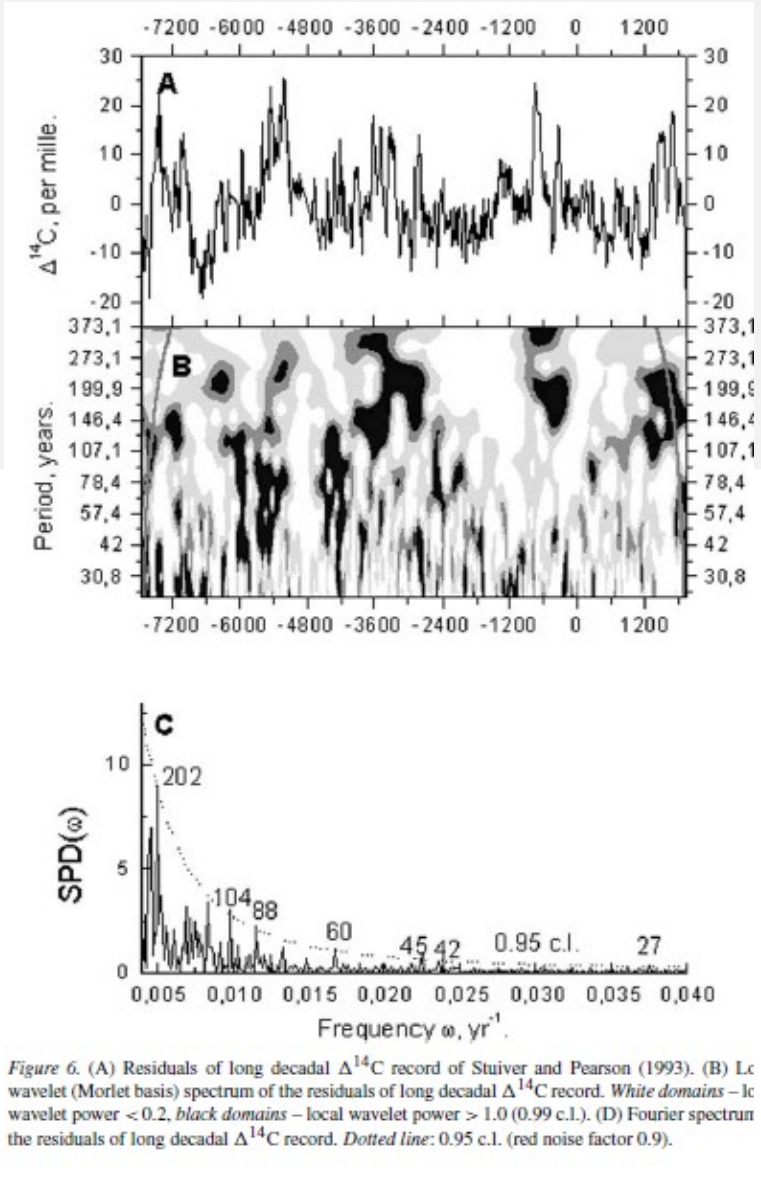

Figure 6. (A) Residuals of long decadal Δ^{14}C record of Stuiver and Pearson (1993). (B) Lo wavelet (Morlet basis) spectrum of the residuals of long decadal Δ^{14}C record. *White domains* – lo wavelet power < 0.2, *black domains* – local wavelet power > 1.0 (0.99 c.l.). (D) Fourier spectrum the residuals of long decadal Δ^{14}C record. *Dotted line*: 0.95 c.l. (red noise factor 0.9).

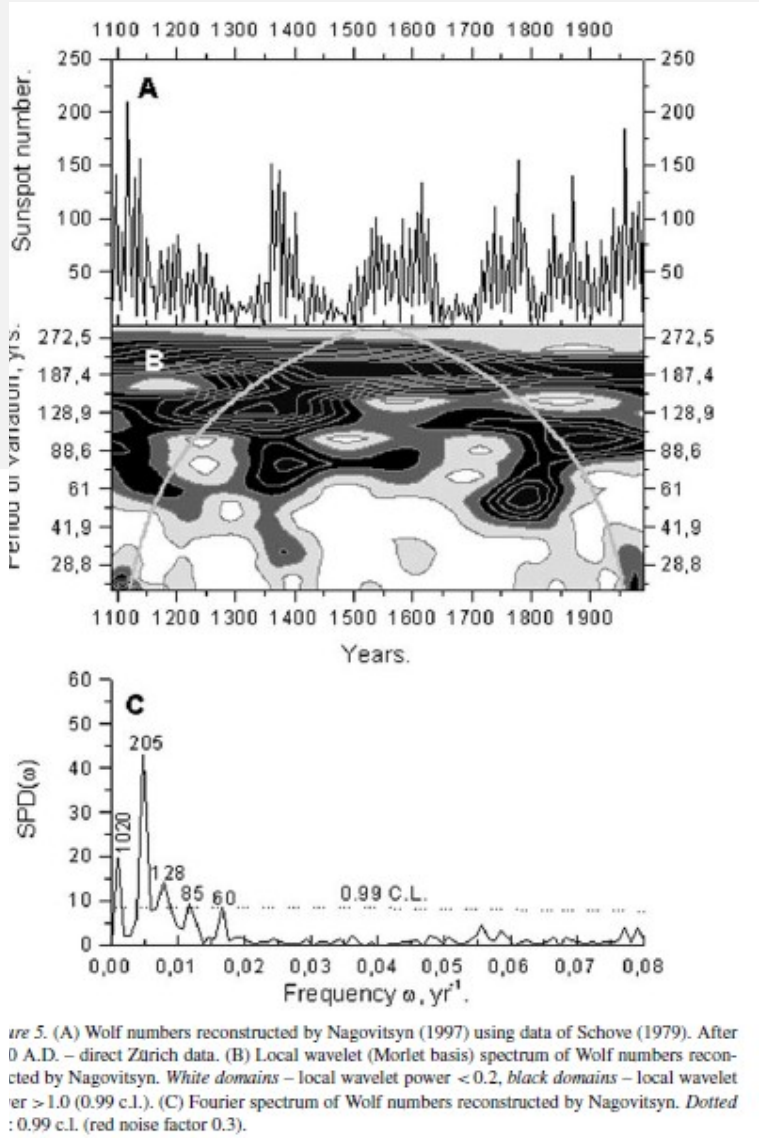

ure 5. (A) Wolf numbers reconstructed by Nagovitsyn (1997) using data of Schove (1979). After 0 A.D. – direct Zürich data. (B) Local wavelet (Morlet basis) spectrum of Wolf numbers recon- cted by Nagovitsyn. *White domains* – local wavelet power < 0.2, *black domains* – local wavelet er > 1.0 (0.99 c.l.). (C) Fourier spectrum of Wolf numbers reconstructed by Nagovitsyn. *Dotted* : 0.99 c.l. (red noise factor 0.3).

A Planetary theory of solar variations

Extract of a Letter from Prof. R. Wolf, of Zurich, to Mr. Carrington, dated Jan. 12, 1859.

(*Translation.*)

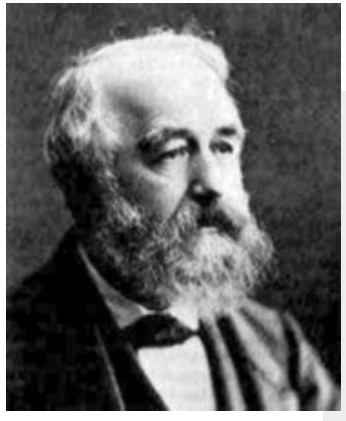

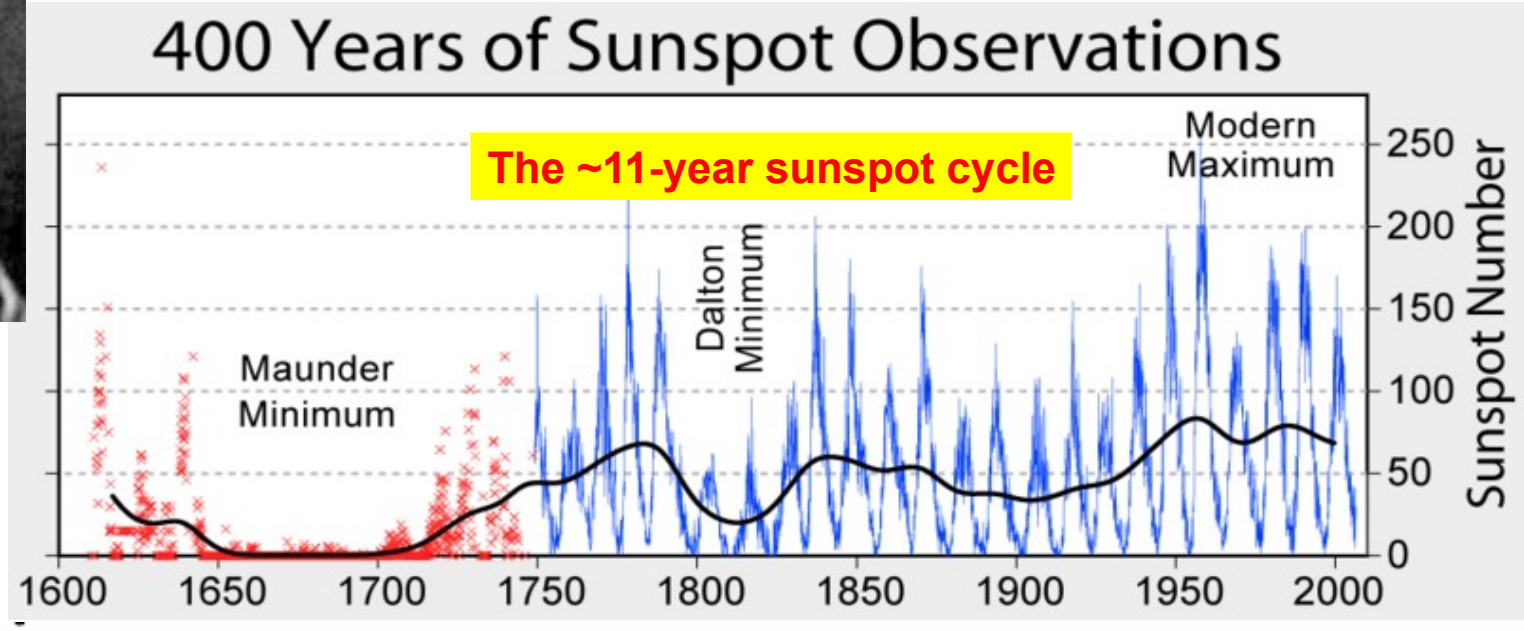

the same planets, the conclusion seems to be inevitable, that my conjecture that the variations of spot-frequency depend on the influences of *Venus, Earth, Jupiter, and Saturn,* will not prove to be wholly unfounded. The preponderating planet

The Sun's Wobbling

- Scafetta, N., 2014. The complex planetary synchronization structure of the solar system.Pattern Recognition in Physics 2, 1-19.

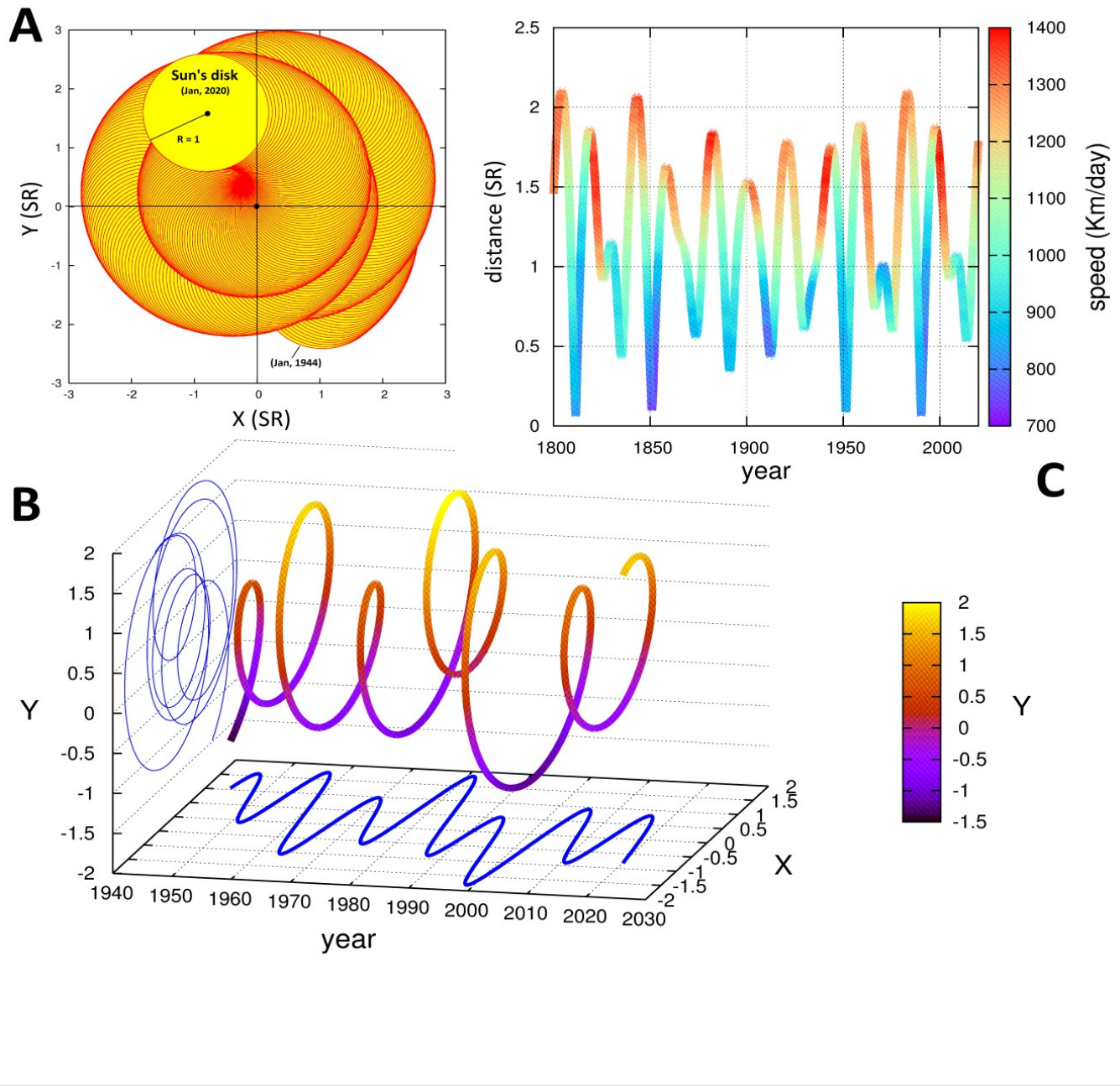

Planetary harmonics of interest

- Orbital periods
- Tidal oscillation due to spring combinations of two or more planets
- Conjunction cycles of two or more planets
- Planetary resonances

The origin of the 11-year solar cycle

- The Venus – Earth – Jupiter model
- The Jupiter – Saturn model

The Venus – Earth – Jupiter model

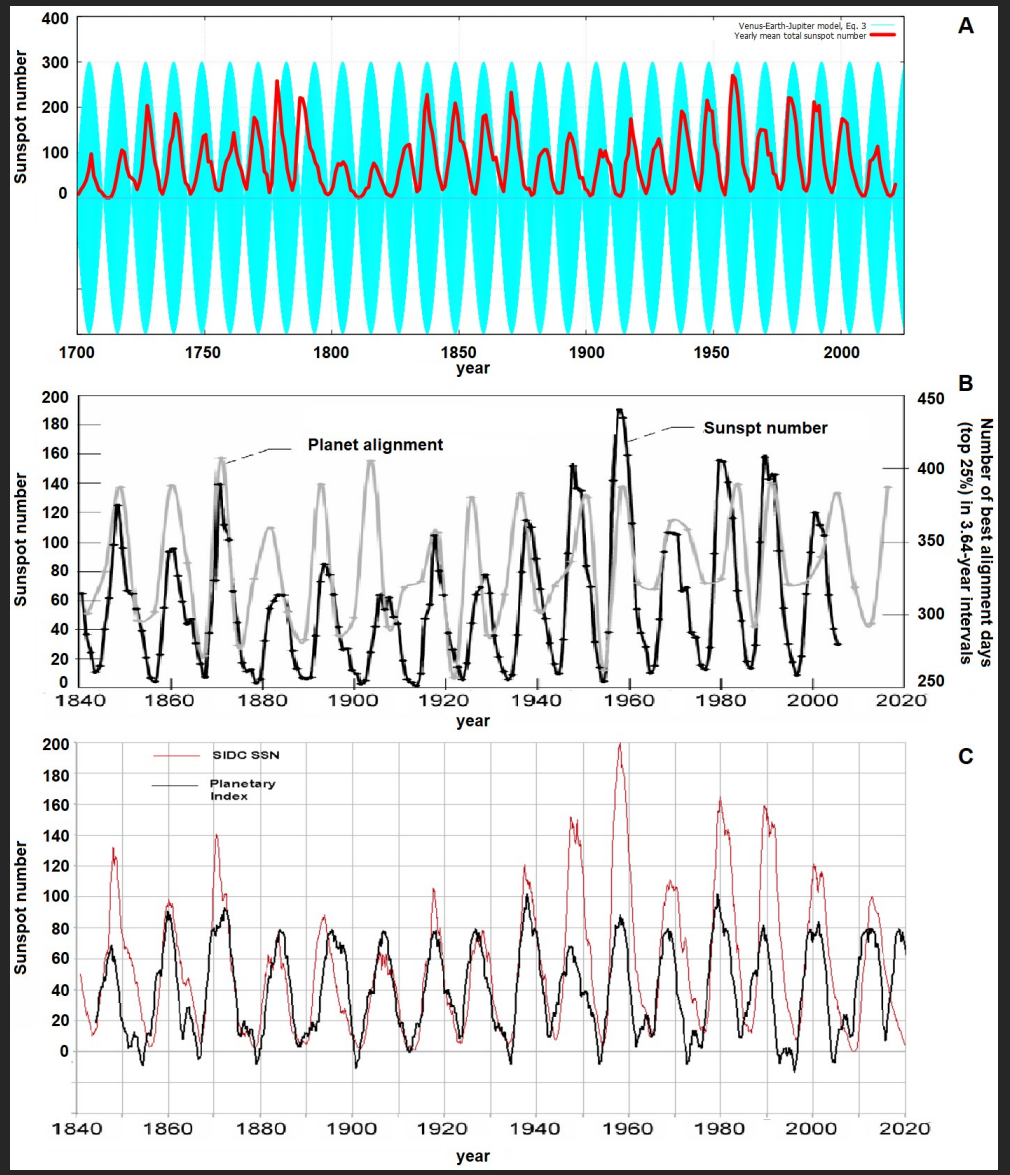

$$f(t) = \cos\left(2\pi \cdot 3\frac{t - t_{VE}}{P_{VE}}\right) + \cos\left(2\pi \cdot 2\frac{t - t_{EJ}}{P_{EJ}}\right)$$

$$P_{VEJ} = \frac{1}{2}\left(\frac{3}{P_V} - \frac{5}{P_E} + \frac{2}{P_J}\right)^{-1} = 11.07\,year$$

The Venus, Earth, and Jupiter triple-syzygies tidal alignment model

The Jupiter – Saturn Tidal model

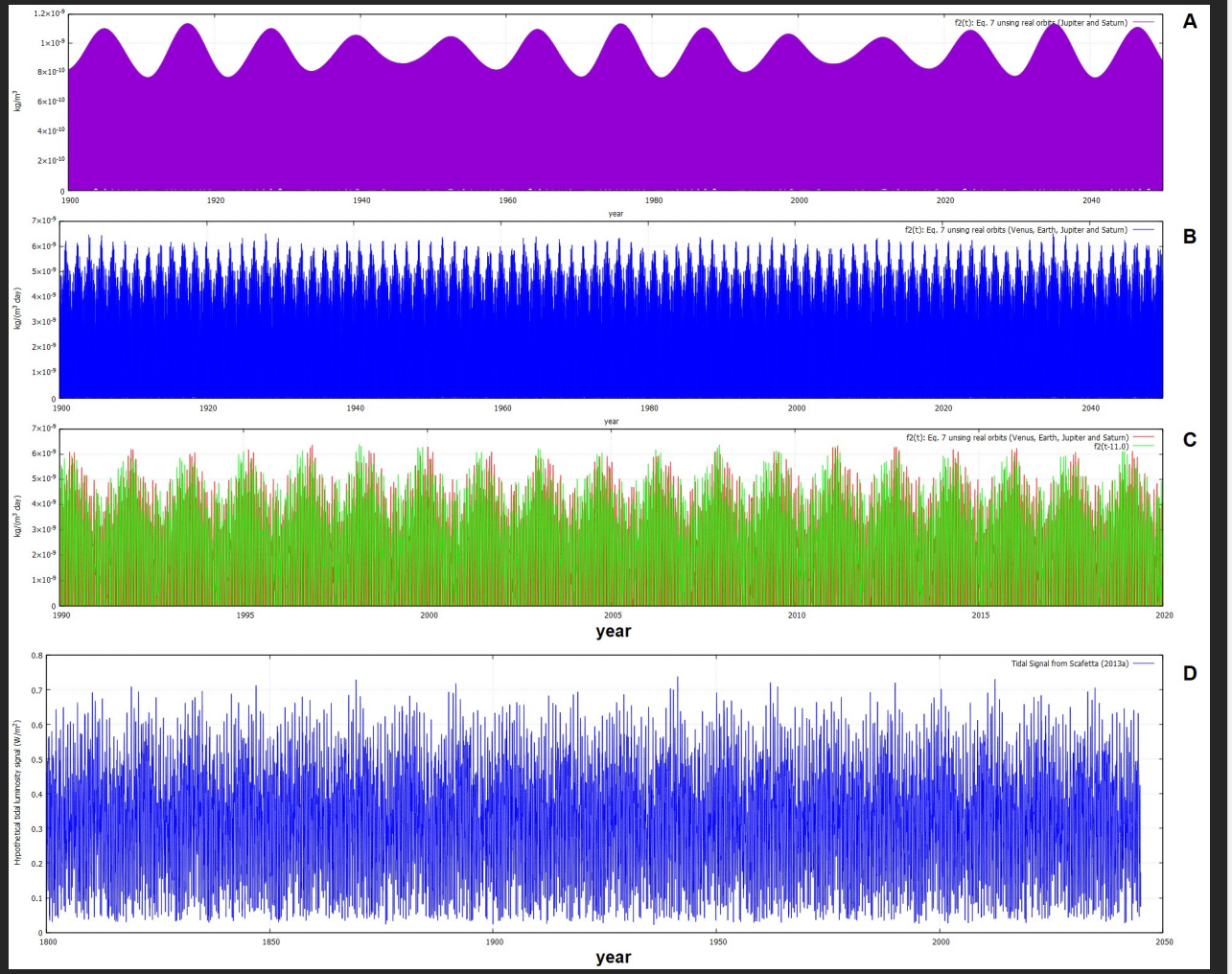

$$Tide_2(t) = \sum_P \frac{m_p}{\left[d_P + (d_{Pa} - d_P)\cos\left(2\pi\frac{t-t_{Pa}}{T_P/365.25}\right)\right]^3} \cdot \left[\cos^2\left(2\pi\frac{t-2000}{T_S/365.25} - 2\pi\frac{t-2000}{T_P/365.25} - 2\pi\frac{\alpha_{PJ,2000}}{360^\circ}\right) - \frac{1}{3}\right],$$

$$f_2(t) = \left|\frac{dTide_2(t)}{dt}\right| \approx \left|\frac{Tide_2(t) - Tide_2(t - 1\,day)}{1\,day}\right|.$$

$$I_P(t) = \frac{3\,G\,R_S^5}{2\,Q\,\Delta t}\int_0^1 K(\chi)\,\chi^4\rho(\chi)\,\mathrm{d}\chi \cdot \int_{\theta=0}^{\pi}\int_{\phi=0}^{2\pi}\left|\sum_{P=1}^{8} mP\frac{\cos^2(\alpha_{P,t}) - \frac{1}{3}}{R_{SP}^3(t)} - mP\frac{\cos^2(\alpha_{P,t-\Delta t}) - \frac{1}{3}}{R_{SP}^3(t-\Delta t)}\right|\sin(\theta)\,\mathrm{d}\theta\mathrm{d}\phi,$$

The Jupiter – Saturn Tidal model

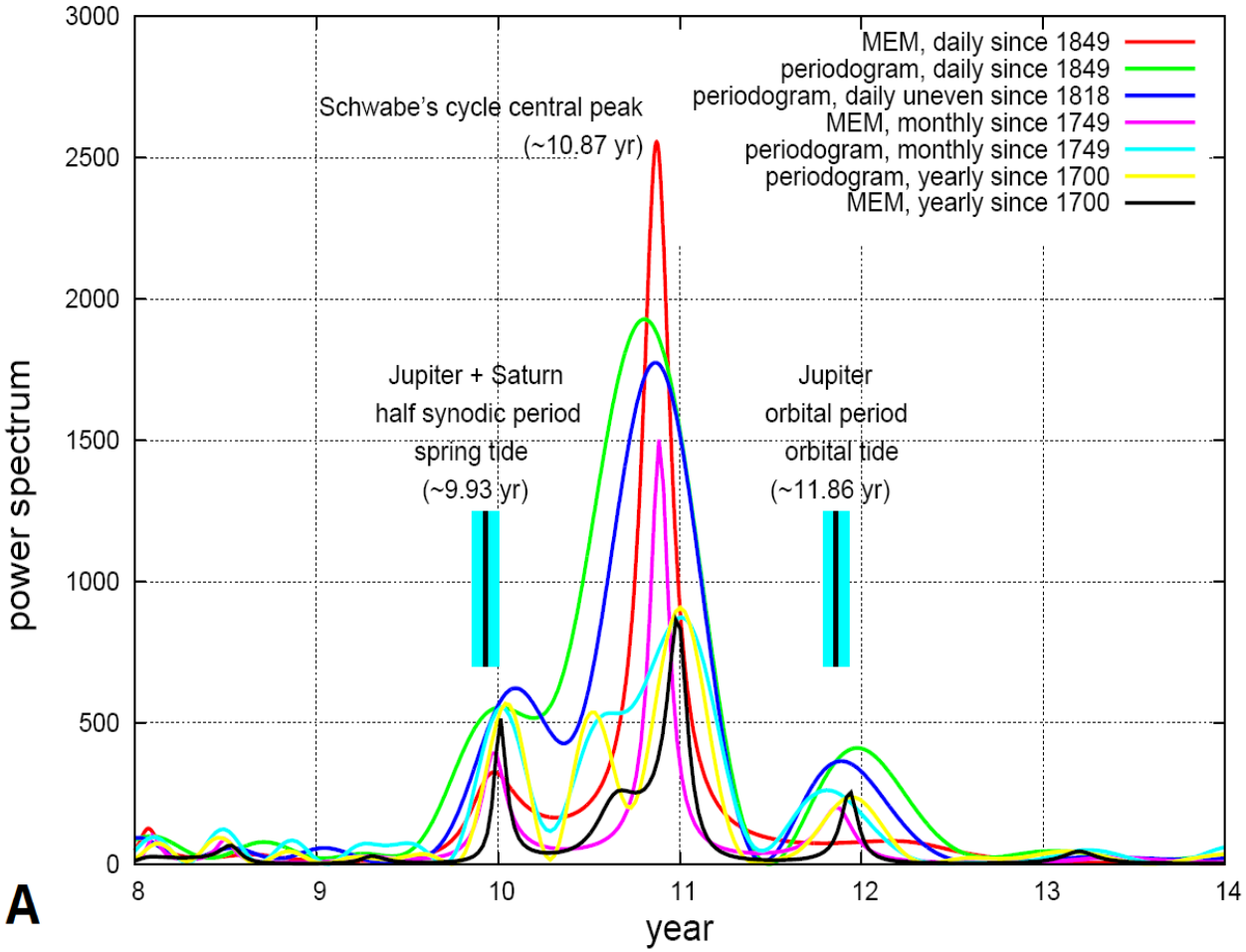

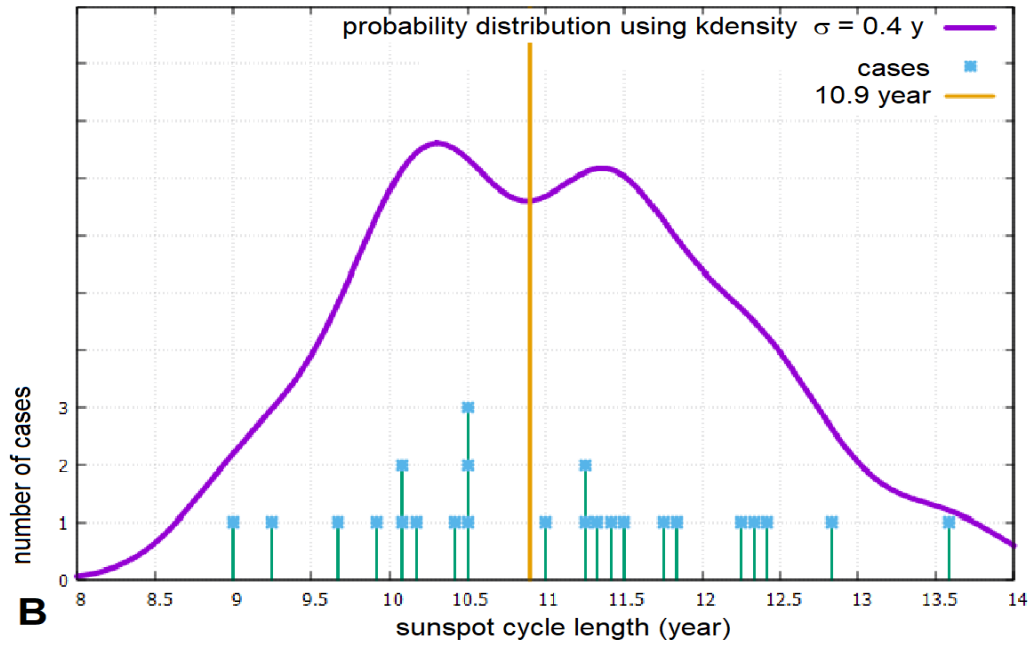

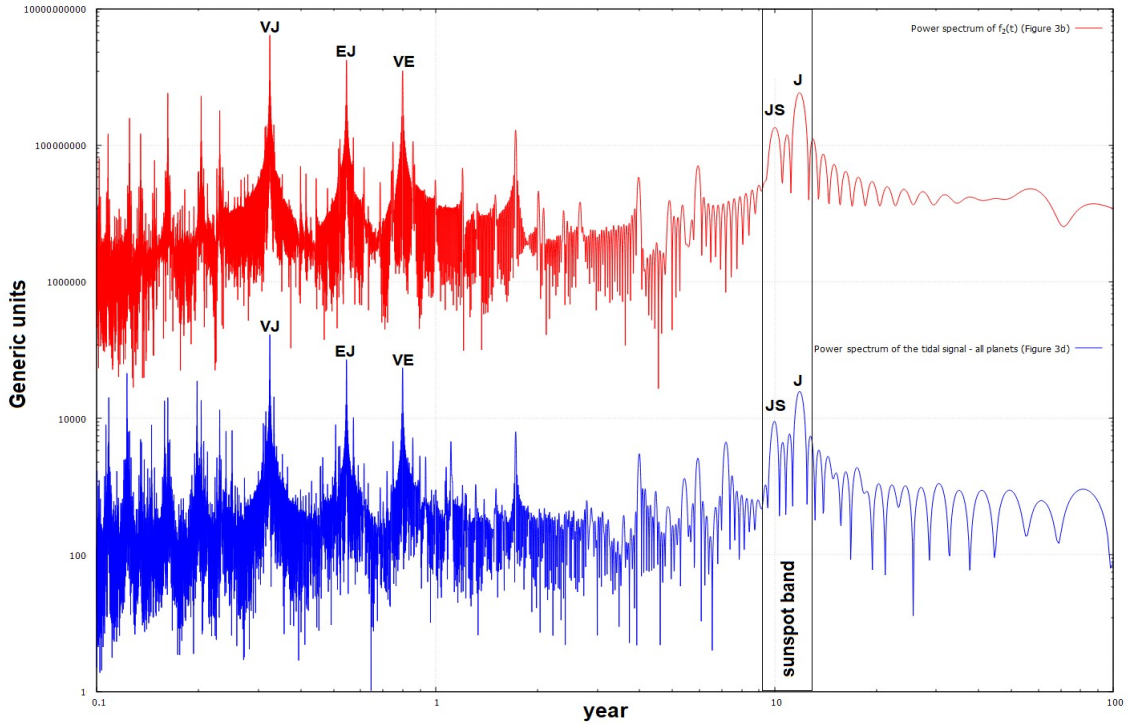

The Venus – Earth – Jupiter –Saturn model

Thus, using the planetary set originally suggested by Wolf (1859), the five strongest tidal spectral peaks are P_{VJ}, P_{EJ}, P_{VE}, P_{SJ} and P_J. As we have seen, the last two (P_{SJ} and P_J) clearly fit the Schwabe 11-year sunspot cycle. Let's now explain the key characteristic of the other three harmonics: P_{VJ}, P_{EJ} and P_{VE}.

The faster tidal oscillations, associated with the spring tides between Venus and Jupiter ($P_{VJ} = 0.3244$ year), Venus and Earth ($P_{VE} = 0.7993$ year) and Earth and Jupiter ($P_{EJ} = 0.5460$ year) exhibit a recurring pattern that requires careful examination. This can be done by looking for combinations of integers η_1,η_2 and η_3 such that the following identity holds

$$P_{JS} < \eta_1 \cdot P_{VJ} \approx \eta_2 \cdot P_{EJ} \approx \eta_3 \cdot P_{VE} < P_J, \tag{9}$$

and the recurrence times are as close to each other as possible. The three best combinations (η_1, η_2, η_3) are $(32, 19, 13) = 10.38 \pm 0.01$ years, $(34, 20, 14) = 11.05 \pm 0.1$ years and $(35, 21, 14) = 11.34 \pm 0.1$ years. Of the three combination sets, the one that is best centered between P_{JS} and P_J is $(34, 20, 14)$. Finally, by averaging all the five main tidal periods, we get

$$\frac{P_{JS} + 34P + 20P_{EJ} + 14P_{VE} + P_J}{5} = 11.0 \pm 0.6\, year. \tag{10}$$

Three-frequency solar harmonic model vs. temperature reconstructions (~61 yr, ~115 yr, ~980 yr cycles)

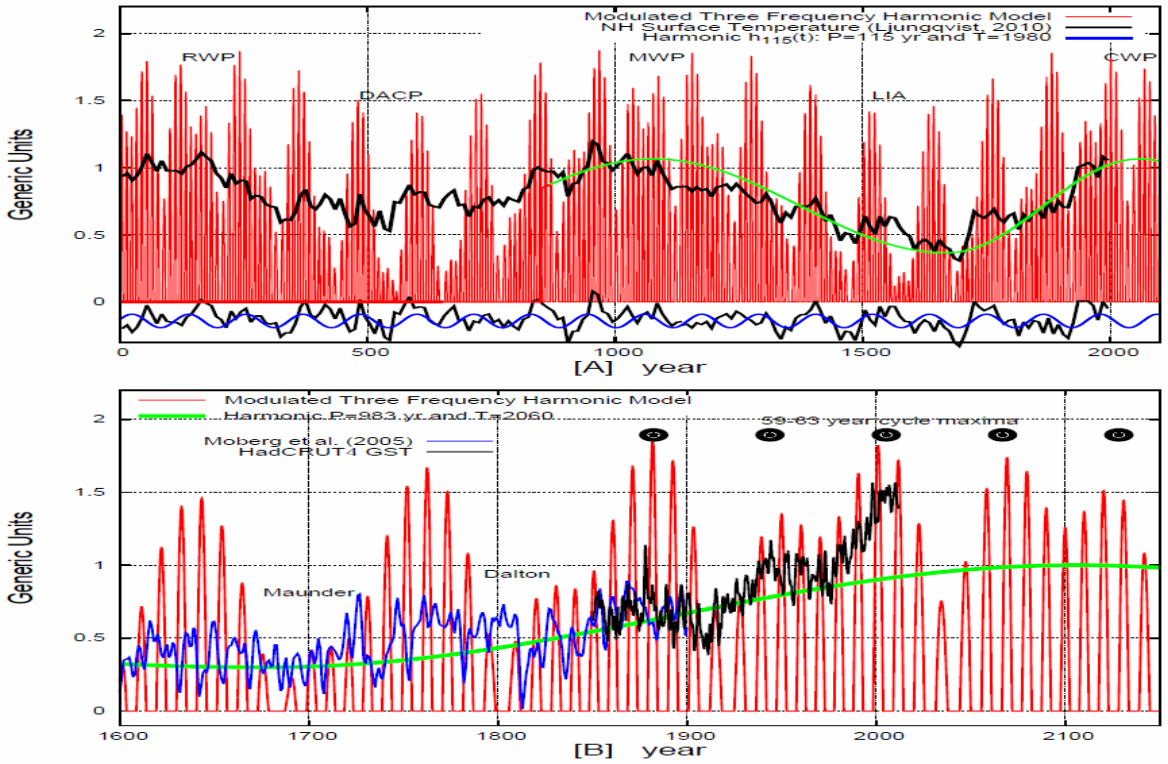

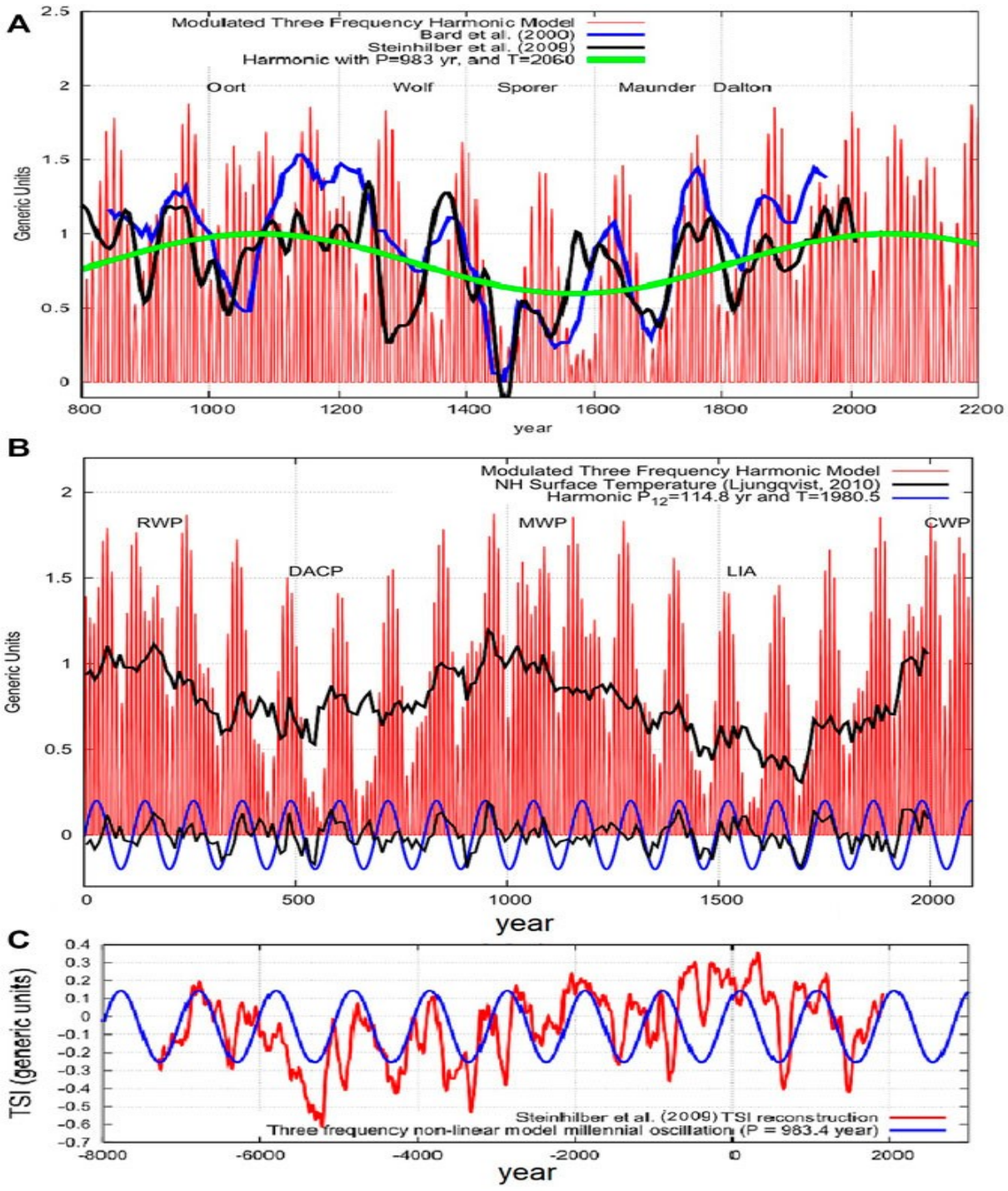

Scafetta N., 2012. Multi-scale harmonic model for solar and climate cyclical variation throughout the Holocene based on Jupiter-Saturn tidal frequencies plus the 11-year solar dynamo cycle. Journal of Atmospheric and Solar-Terrestrial Physics 80, 296-311.

Monthly to the annual timescales

The figure demonstrates that the TSI periodogram contains all the primary spring and synodic planetary harmonics from the monthly to

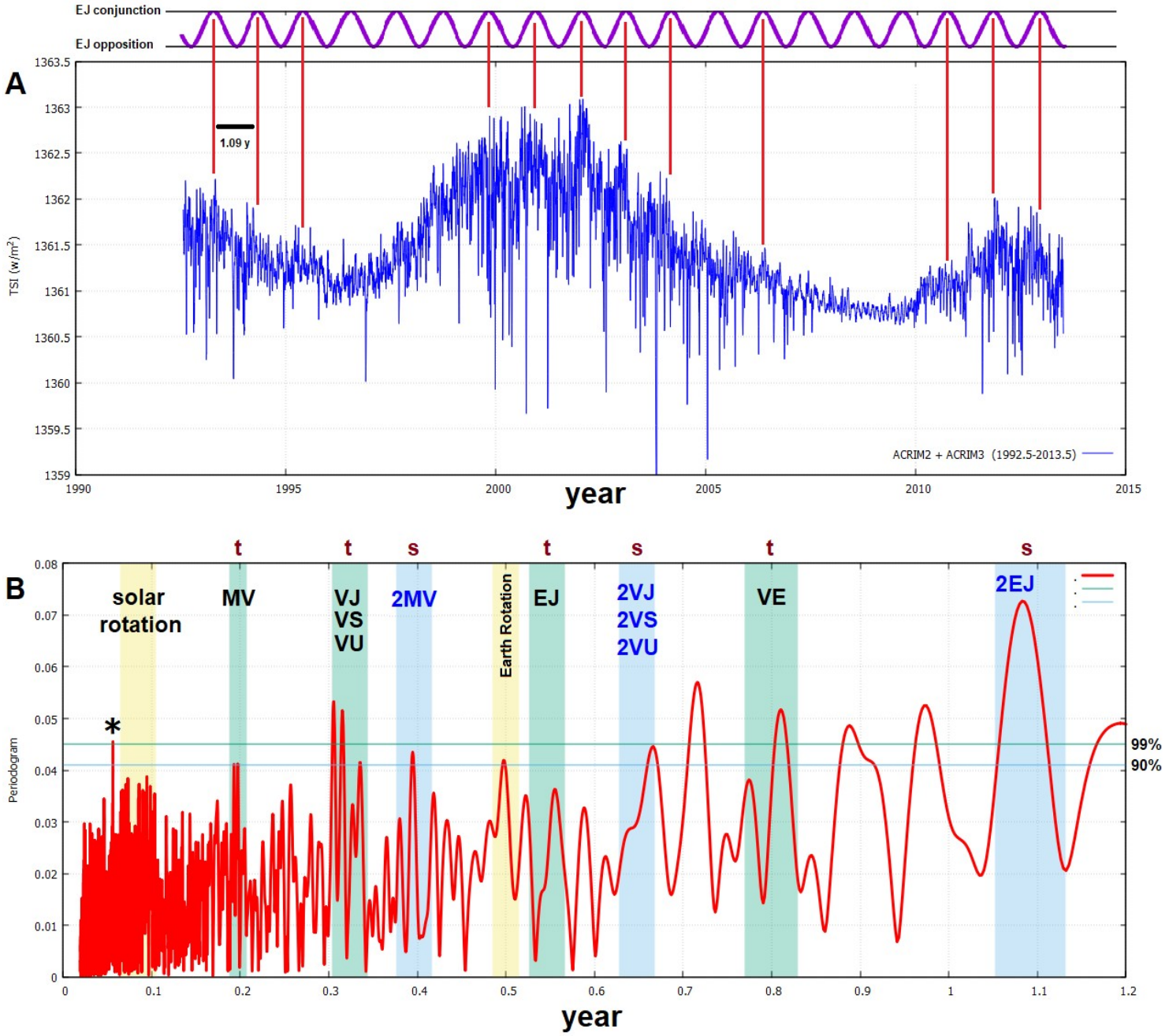

Empirical evidences for a planetary modulation of total solar irradiance and the TSI signature of the 1.09-year Earth-Jupiter conjunction cycle.

Scafetta N., and R. C. Willson, Astrophysics and Space Science (2013).

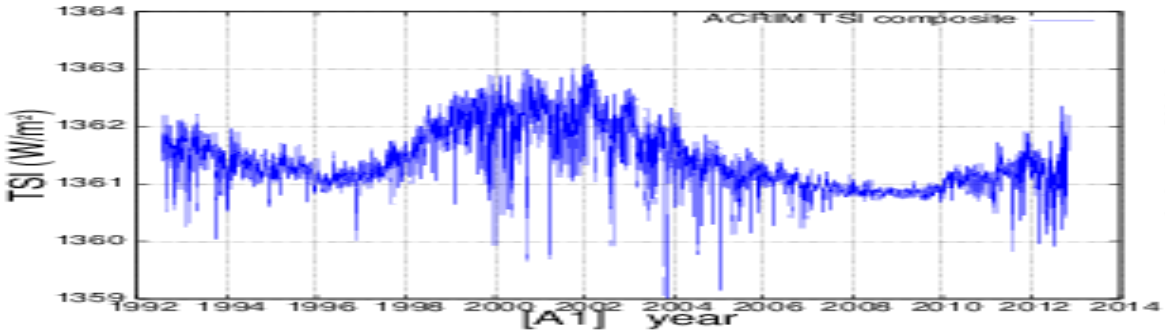

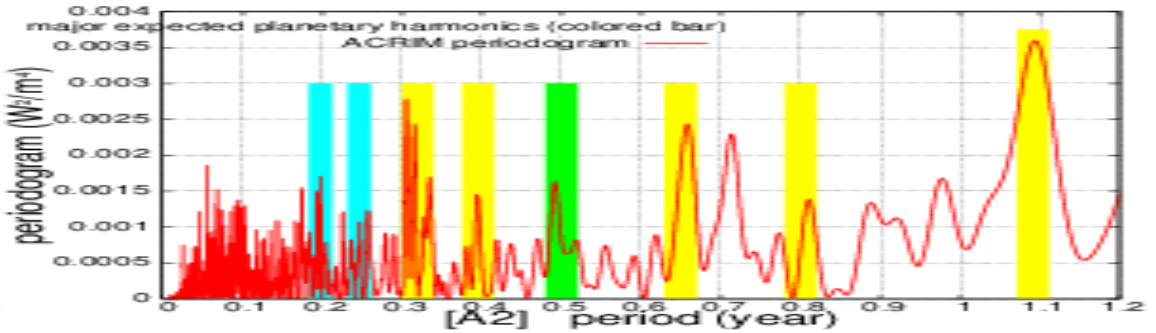

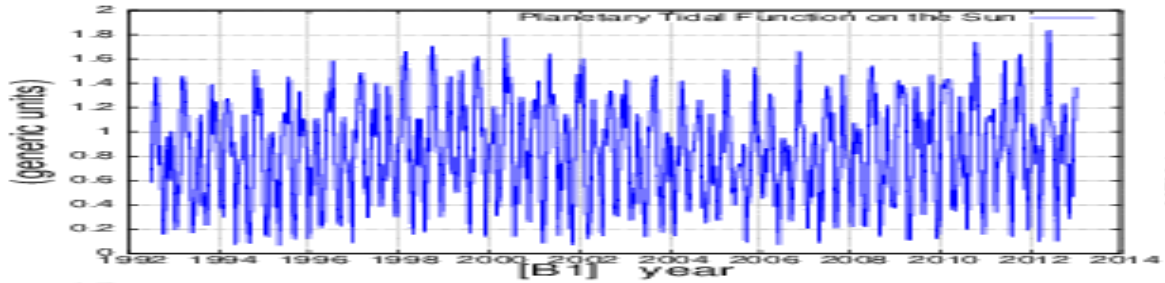

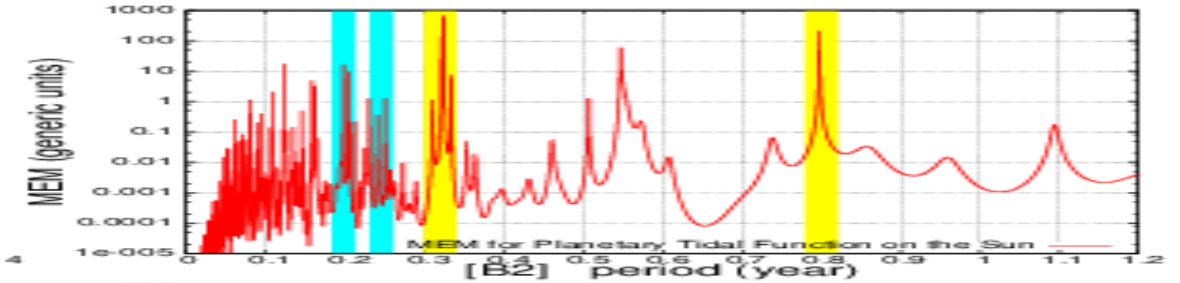

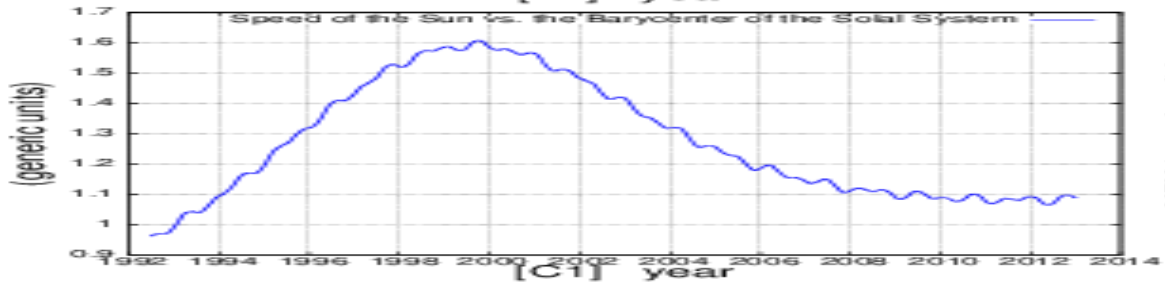

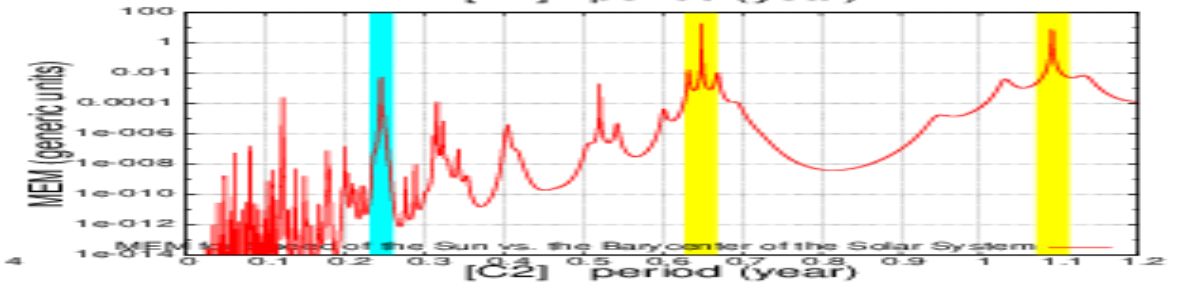

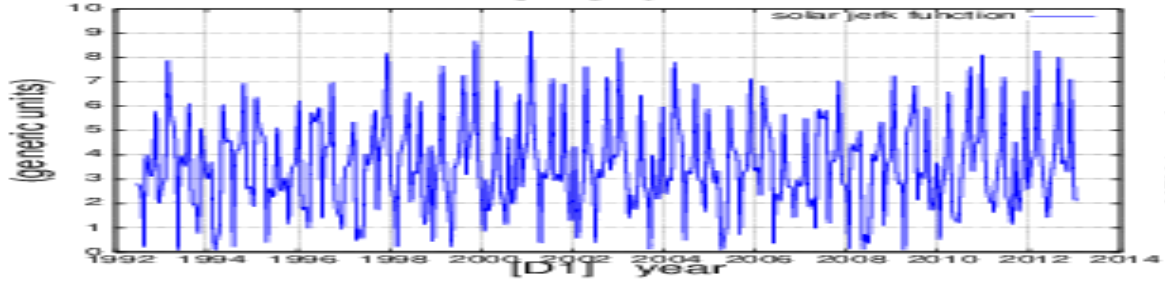

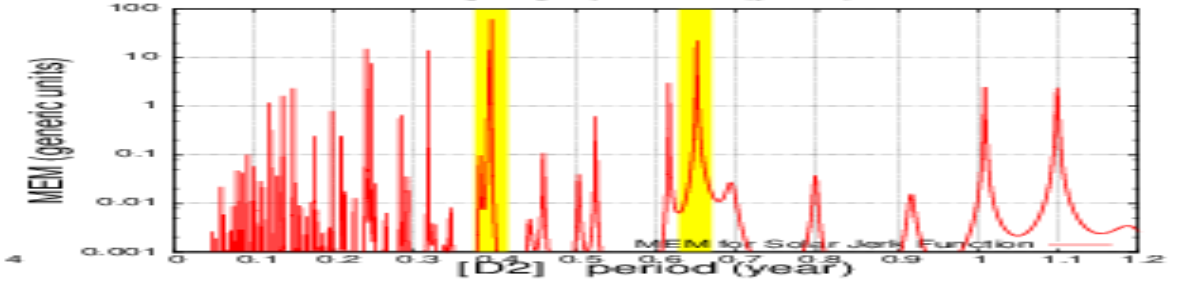

The Sun's side toward Jupiter is brighter!

Scafetta N., and R. C. Willson, 2013. Empirical evidences for a planetary modulation of total solar irradiance and the TSI signature of the 1.09-year Earth-Jupiter conjunction cycle. Astrophysics and Space Science 348(1), 25-39.

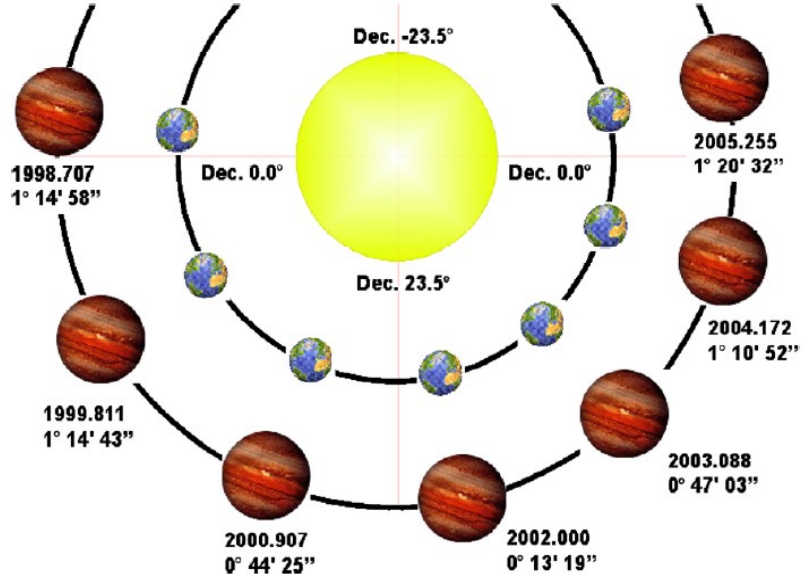

Fig. 3 The Earth-Jupiter conjunction cycle (1.09-year) during solar cycle 23 maximum (1998–2004)

Fig. 5 [A] ACRIM and [B] PMOD TSI satellite composites since 1978 (*red*). The *blue curves* are 2-year moving average smooth, $S_A(t)$ and $S_P(t)$, for ACRIM and PMOD respectively. The *black curves* are empirical representations of Earth-Jupiter conjunction 1.092-year cycle modulated by the 11-year solar cycle. The modeled curves are approximations used only for visualization purpose: see Eqs. (7) and (8)

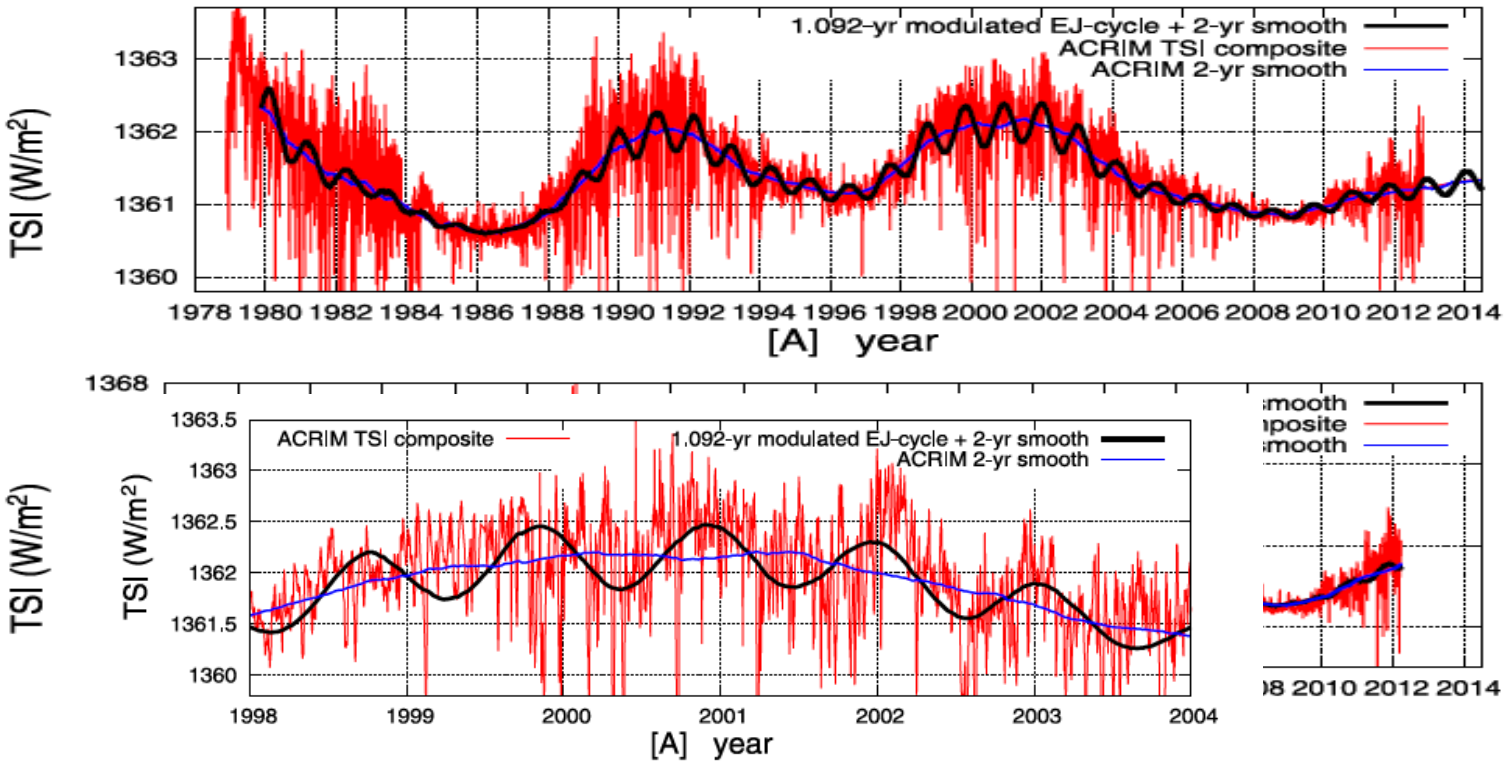

Scafetta, N., Milani, F., Antonio Bianchini, A., Ortolani, S.: 2016. On the astronomical origin of the Hallstatt oscillation found in radiocarbon and climate records throughout the Holocene. Earth-Science Reviews 162, 24–43.

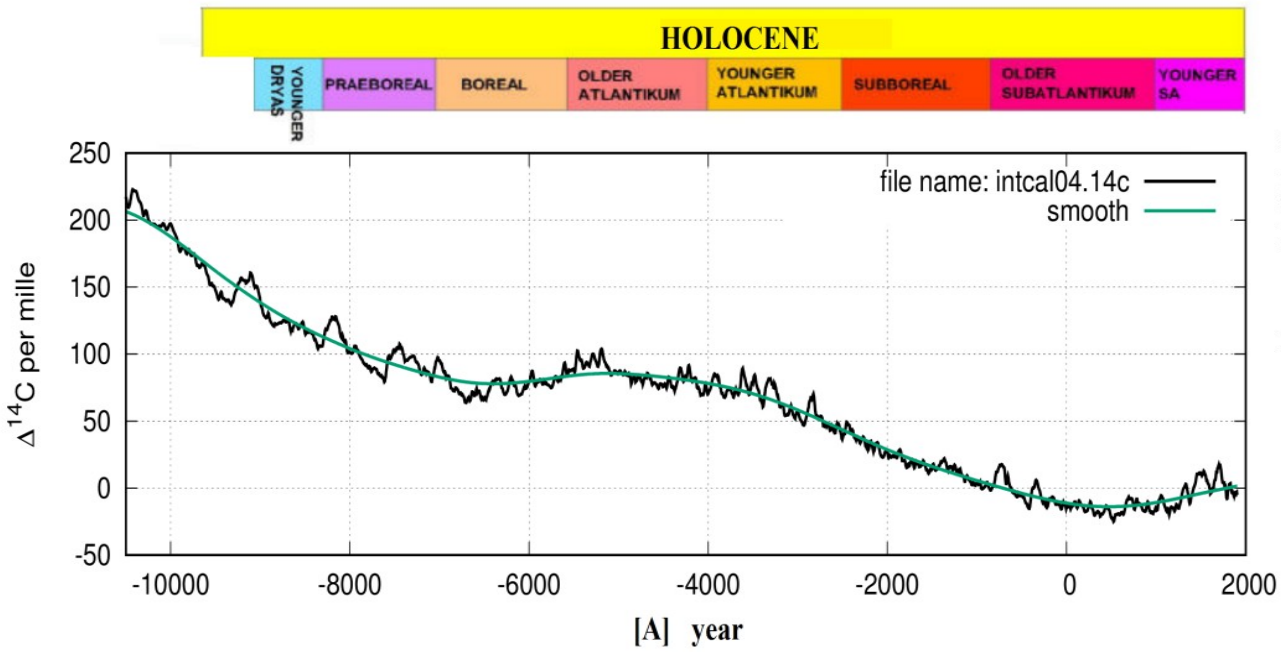

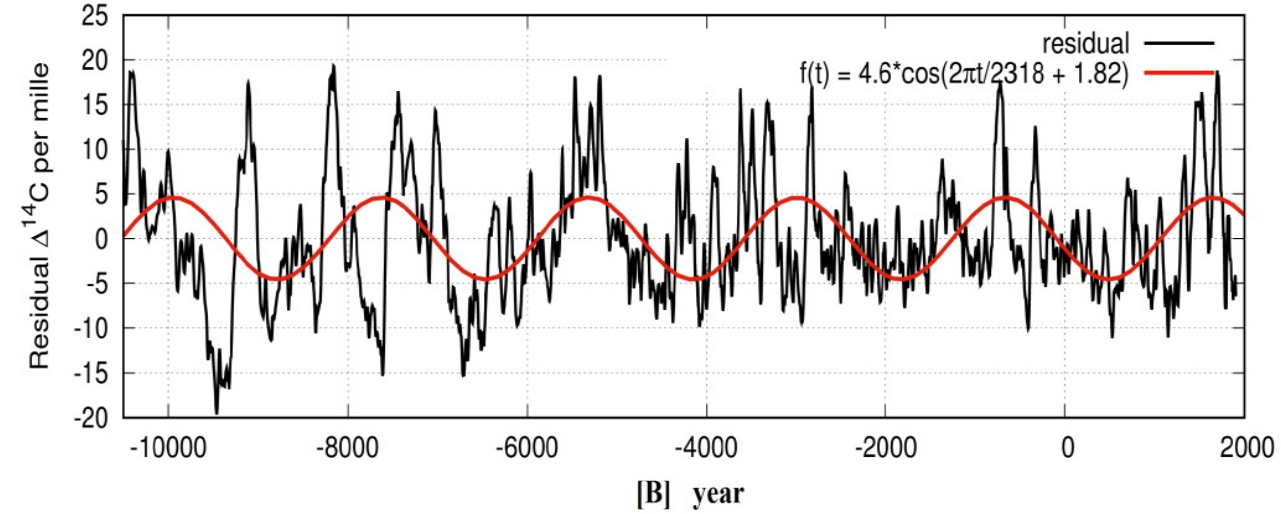

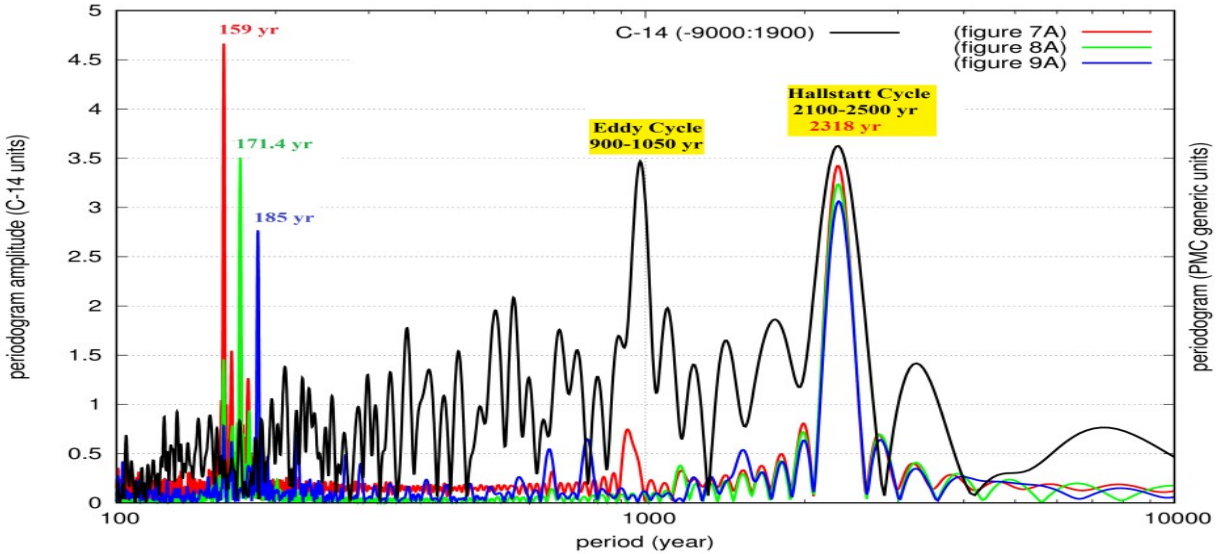

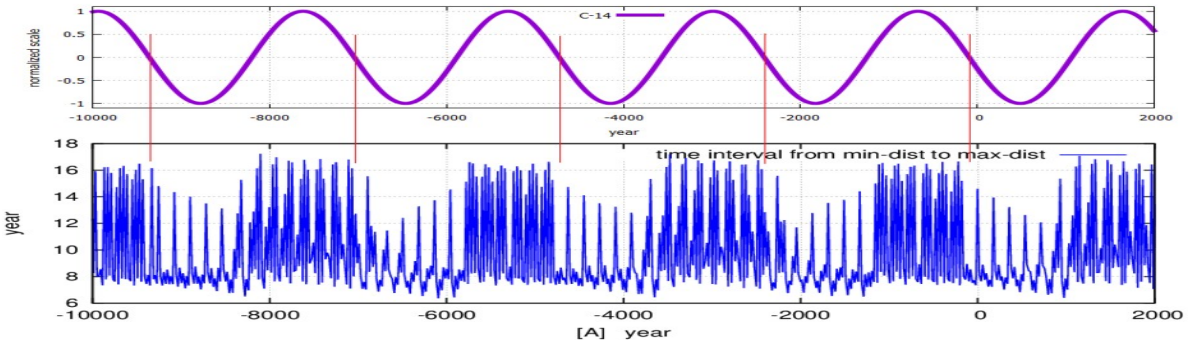

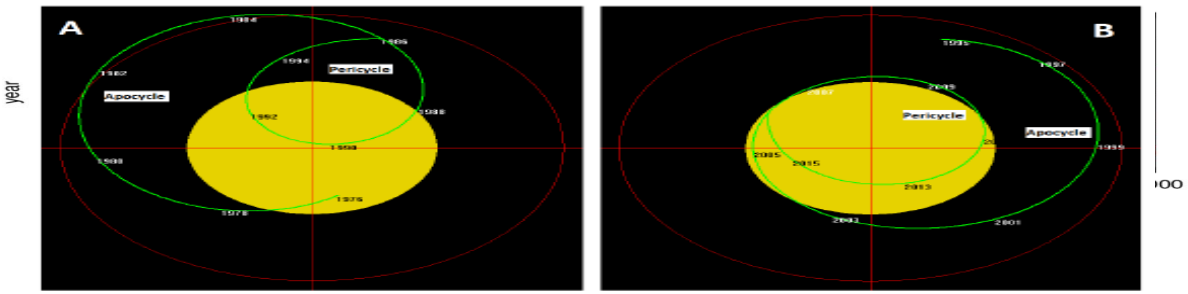

Planetary mass center eccentricity variation & the stable orbital resonances of the Jupiter-Saturn-Uranus-Neptune system

Scafetta et al. in press

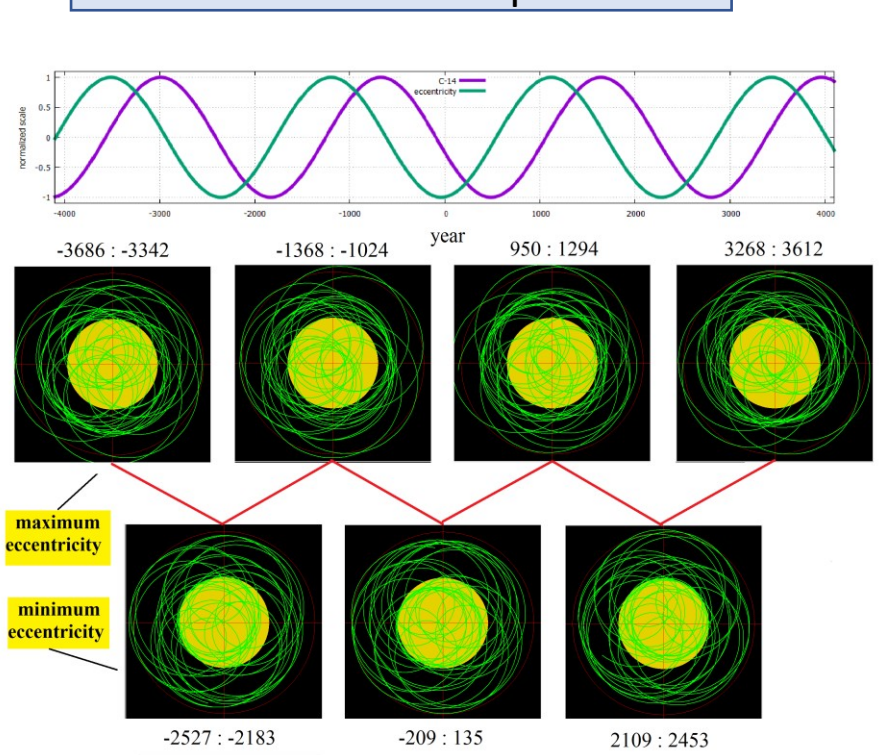

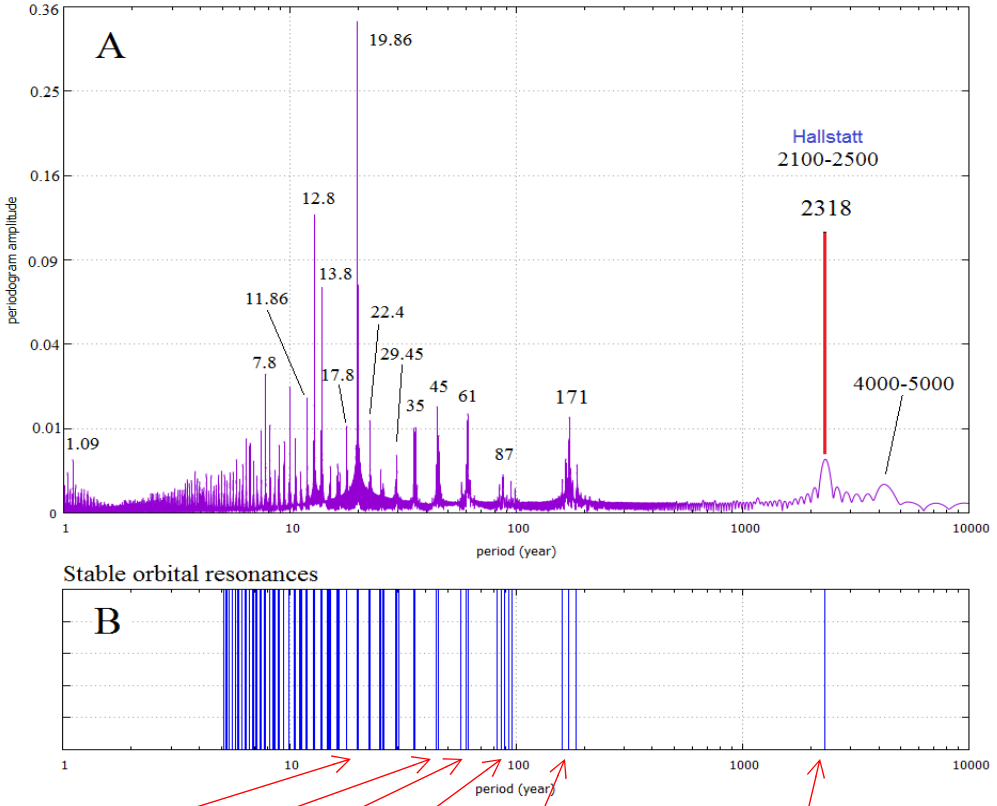

Invariant Inequalities

20 yr | 44-45 yr | 57-61 yr | 82-96 yr | 159-171-185 yr | 2318 yr

Gleissberg | Jose | HallStatt

Conjunctions and asymmetry of the gravitational field of the solar system in an ideal planetary model made up of a central sun and 4 equal large gas planets.

$$f_{12} = \frac{1}{T_{12}} = \left| \frac{1}{T_1} - \frac{1}{T_2} \right|$$

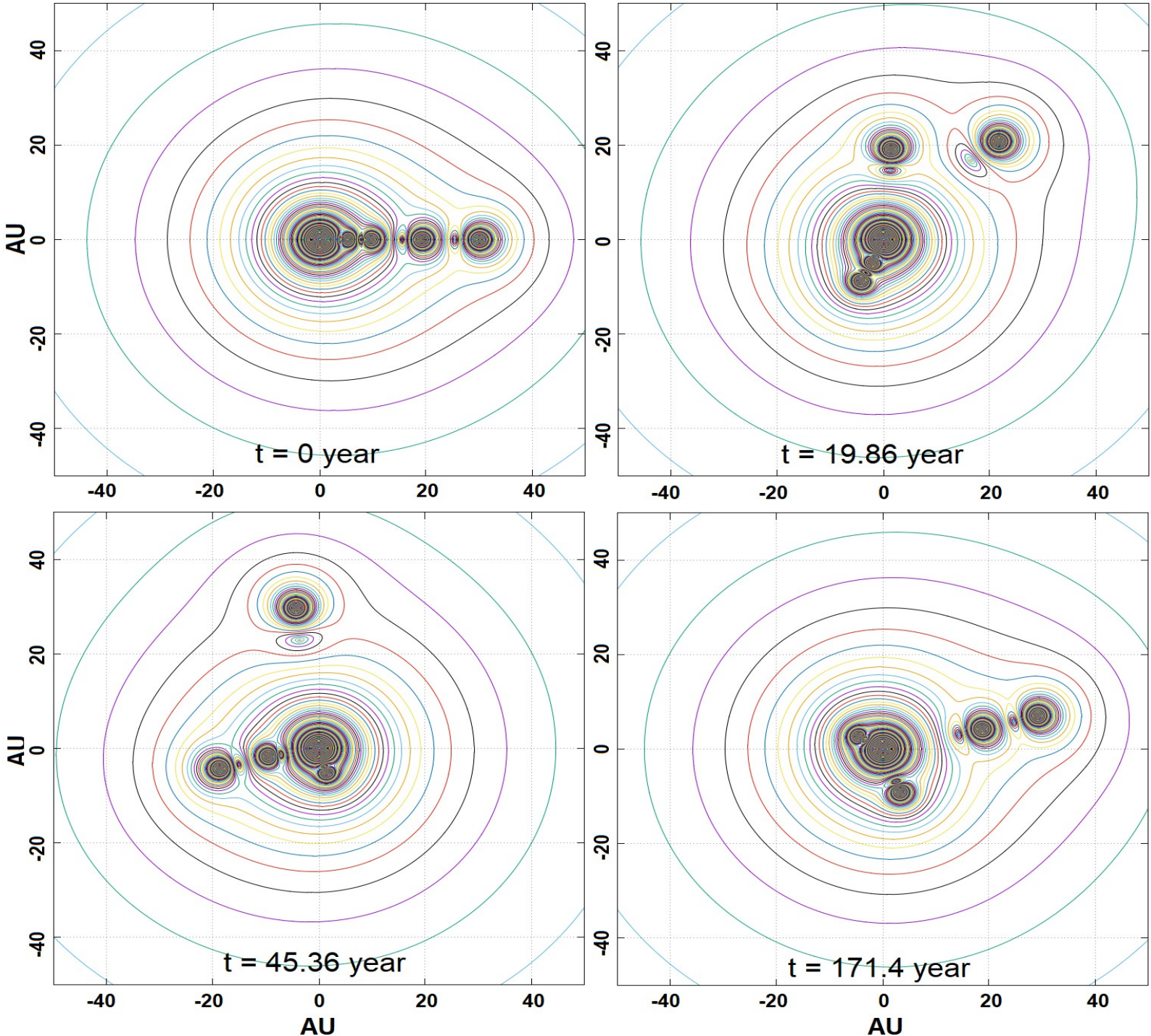

The Planetary Invariant Inequalities

$$f = \frac{1}{T} = \left| \sum_{i=1}^{n} \frac{a_i}{T_i} \right|$$

$$\sum_{i=1}^{n} a_i = 0$$

$$f_i' = \frac{1}{T_i'} = \frac{1}{T_i} - \frac{1}{P}$$

$$f' = \frac{1}{T'} = \left| \sum_{i=1}^{n} \frac{a_i}{T_i} \right| = \left| \sum_{i=1}^{n} \frac{a_i}{T_i} - \frac{\sum_{i=1}^{n} a_i}{P} \right|$$

(Jup, Sat, Ura, Nep)	(M, K)	T (year)	cluster
(1, −3, 5, −3)	(5, 6)	42.1	~45 yr
(0, 0, 4, −4)	(4, 4)	**42.8**	
(2, −5, 1, 2)	(5, 5)	43.7	
(1, −3, −3, 5)	(5, 6)	43.7	
(1, −2, 0, 1)	(2, 2)	**44.5**	
(0, 1, −1, 0)	(1, 1)	**45.4**	
(1, −4, 2, 1)	(4, 4)	**46.3**	
(1, −1, −5, 5)	(5, 6)	47.2	
(1, −3, 4, −2)	(4, 5)	55.8	~60 yr
(0, 0, 3, −3)	(3, 3)	**57.1**	
(2, −5, 0, 3)	(5, 5)	58.6	
(1, −3, −2, 4)	(4, 5)	58.6	
(1, −2, −1, 2)	(2, 3)	**60.1**	
(0, 1, −2, 1)	(2, 2)	**61.7**	
(1, −4, 3, 0)	(4, 4)	**63.4**	
(1, −3, 3, −1)	(3, 4)	**82.6**	Gleissberg
(0, 0, 2, −2)	(2, 2)	**85.7**	
(2, −5, −1, 4)	(5, 6)	89.0	
(1, −3, −1, 3)	(3, 4)	**89.0**	
(1, −2, −2, 3)	(3, 4)	**92.5**	
(0, 1, −3, 2)	(3, 3)	**96.4**	
(1, −4, 4, −1)	(4, 5)	100.6	
(1, −3, 2, 0)	(3, 3)	**159.6**	Jose
(0, 0, 1, −1)	(1, 1)	**171.4**	
(2, −5, −2, 5)	(5, 7)	185.1	
(1, −3, 0, 2)	(3, 3)	**185.1**	
(1, −2, −3, 4)	(4, 5)	**201.1**	Suess–de Vries
(0, 1, −4, 3)	(4, 4)	**220.2**	
(1, −4, 5, −2)	(5, 6)	243.4	
(0, 1, −5, 4)	(5, 5)	**772.7**	Eddy
(1, −2, −4, 5)	(5, 6)	**1159**	
(1, −3, 1, 1)	(3, 3)	**2318**	Bray–Hallstatt

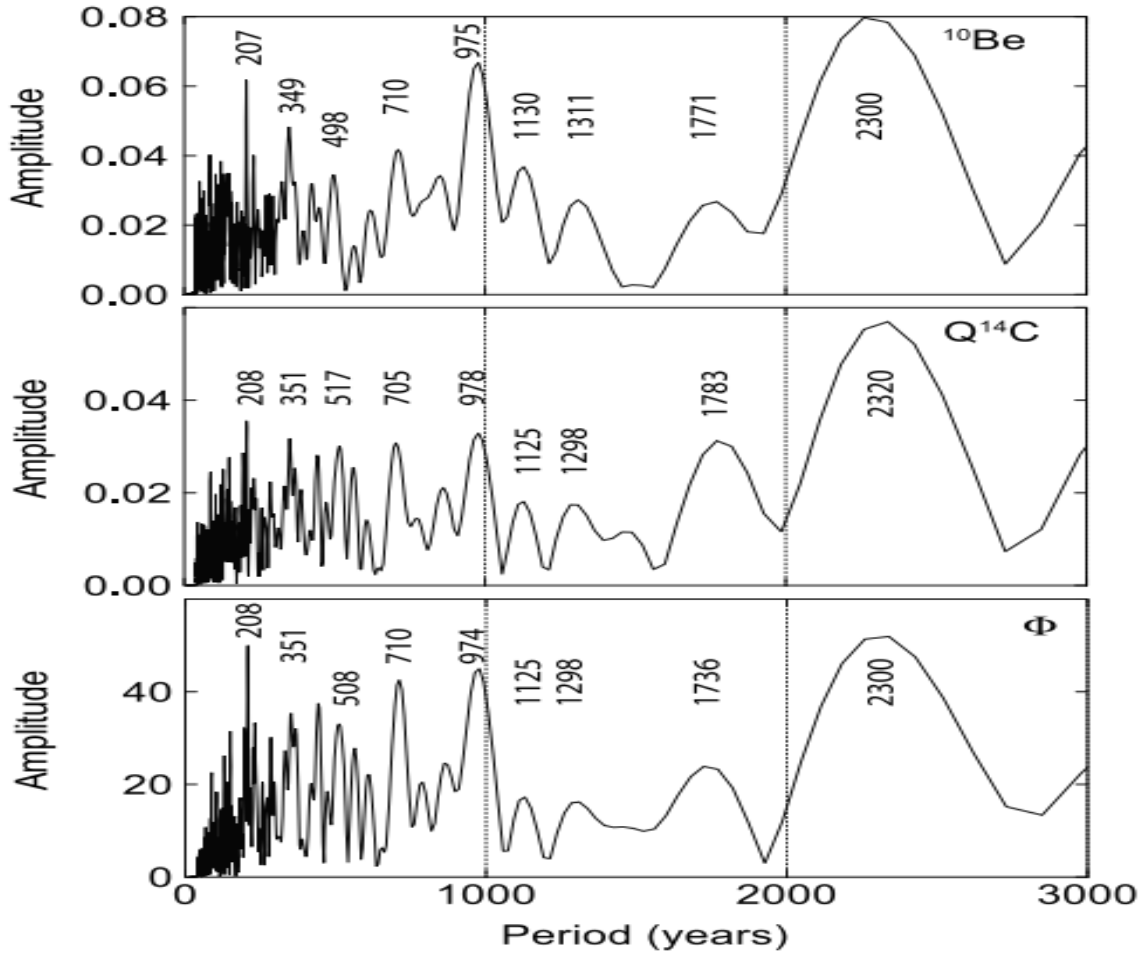

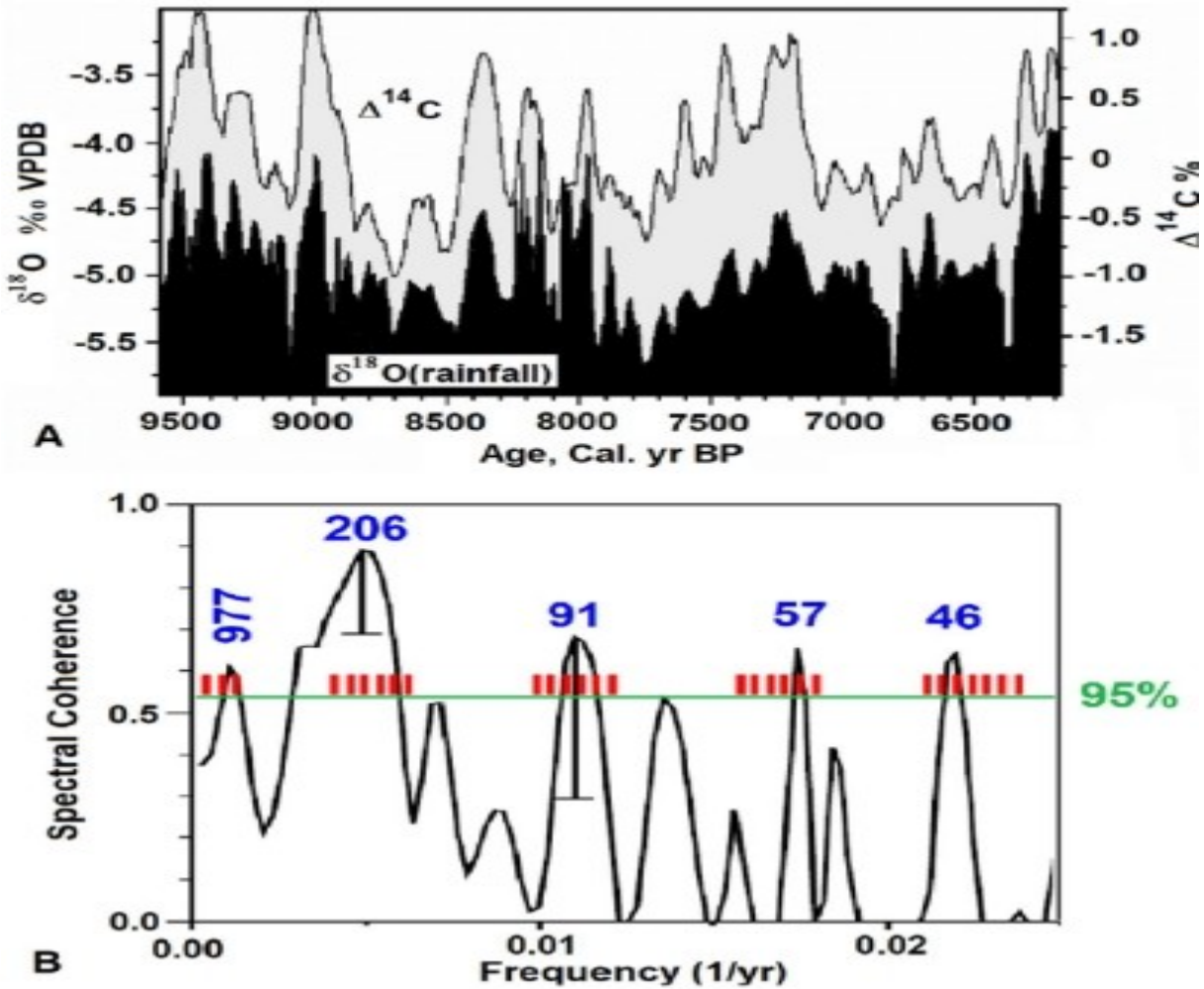

Cycles of Bray – Hallstatt (2100–2500 yr), Eddy (800–1200 yr), Suess – de Vries (200–250 yr), Jose (155–185 yr), Gleissberg (80–100 yr), cluster 55–65 yr, cluster 40-50 yr
McCracken et al. (2013); Neff et al. (2001).

Evidences that the climate system is regulated by astronomical oscillations

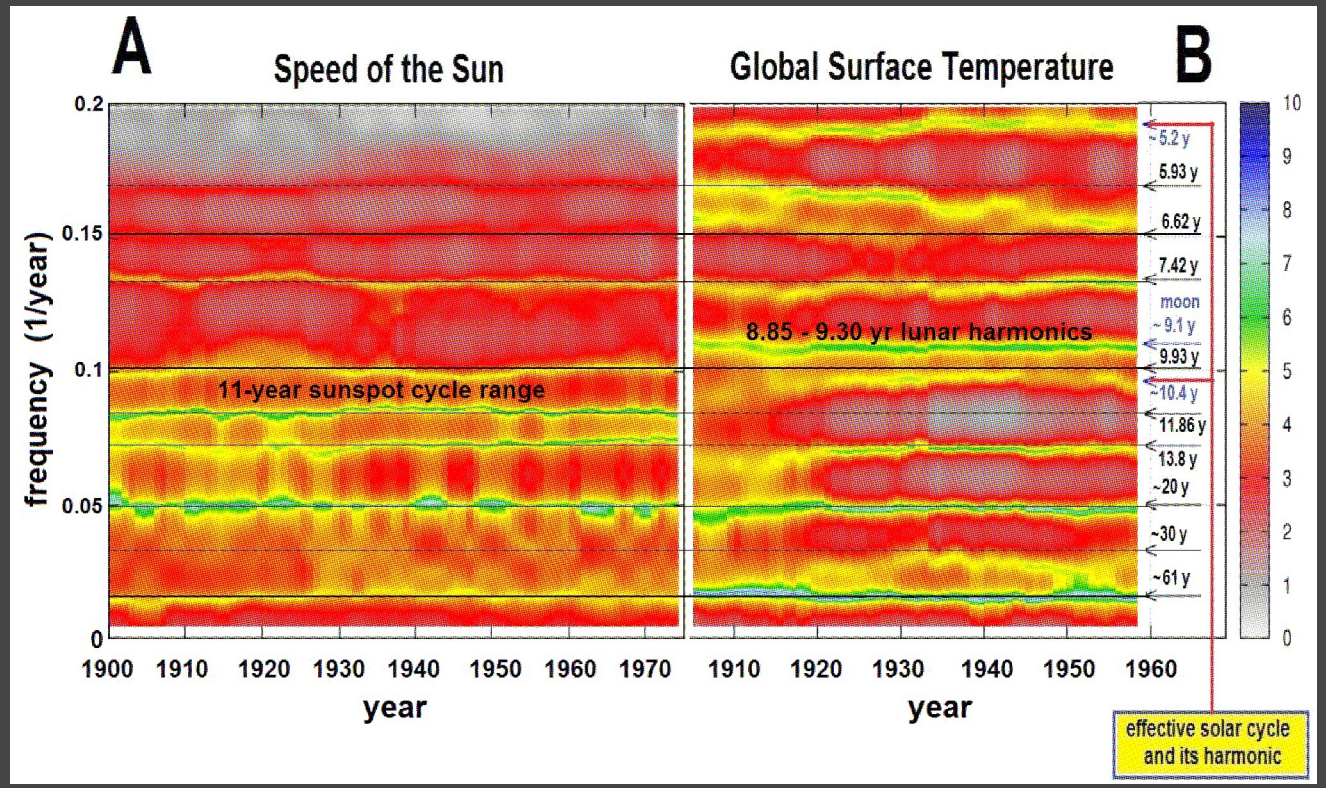

- Scafetta, N., "Discussion on the spectral coherence between planetary, solar and climate oscillations: a reply to some critiques." *Astrophysics and Space Science*, vol. 354, pp. 275-299, 2014.

Interpretation of the 20-60 year frequency band of the Earth's temperature

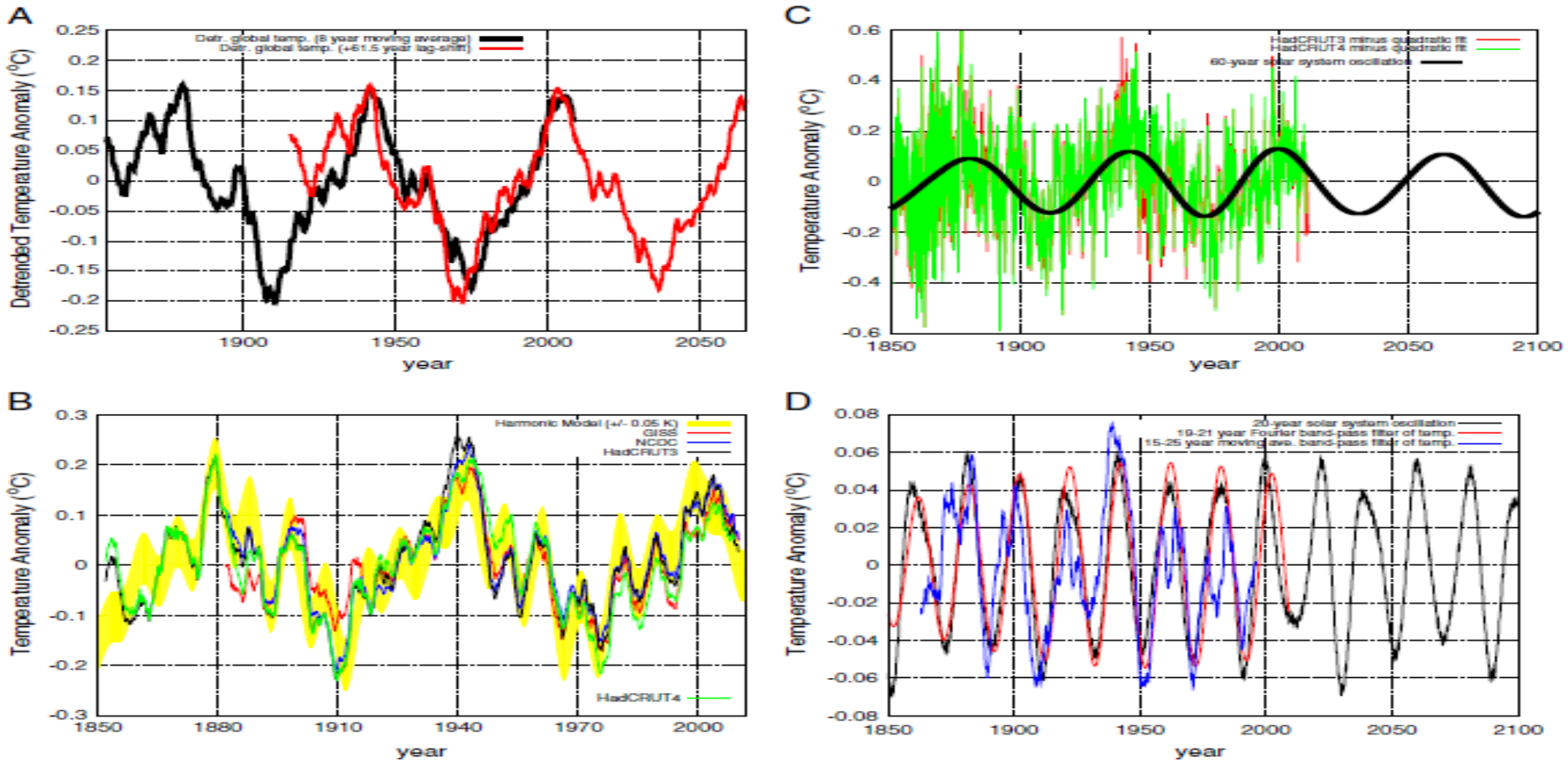

Fig. 3. [A] 8-year moving average of the detrended HadCRUT4 GST plotted against itself with a 61.5-year lag shift (red). The quadratic fitting trend applied is $f(t) = 0.0000298 * (t - 1850)^2 - 0.384$. [B] Four GST records (HadCRUT3, HadCRUT4, GISS and NCDC) after being detrended of their upward trend, and smoothed with a 49-month moving average algorithm against the 4-frequency harmonic model (yellow area) proposed in Scafetta (2010, 2012a,c). [C] and [D] show the HadCRUT records detrended of their warming trend and band-pass filtered to highlight their quasi bi-decadal oscillation. The two black oscillating curves with periods of about 20 years and 60 years are two major astronomical oscillations of the solar system induced by Jupiter and Saturn (Scafetta, 2010).

Harmonic Climate Model

$$H(t) = h_{983}(t) + h_{115}(t) + h_{60}(t) + h_{20}(t) + h_{10.4}(t) + h_{9.1}(t) + \beta * m(t) + const,$$

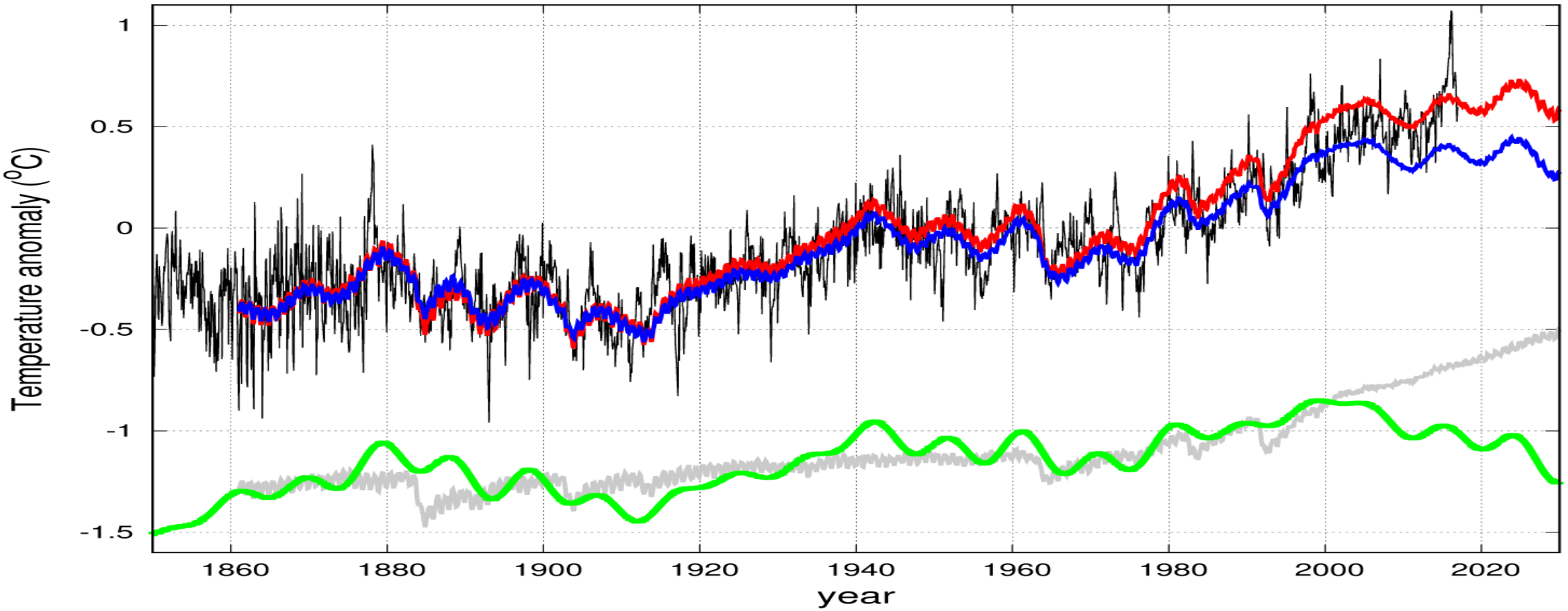

Scafetta, N. 2013. Discussion on climate oscillations: CMIP5 general circulation models versus a semi-empirical harmonic model based on astronomical cycles. Earth-Science Reviews 126, 321-357.

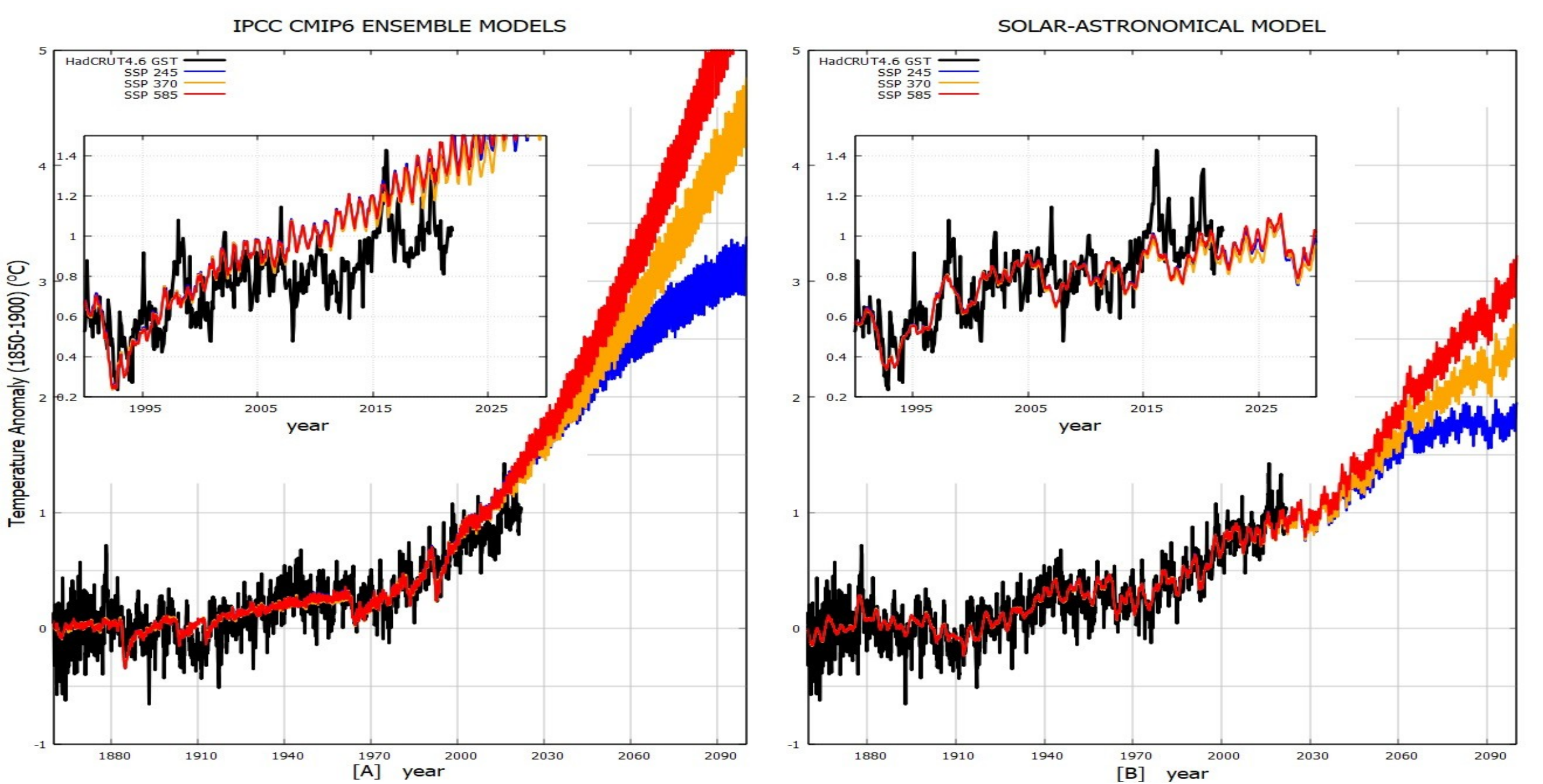

Update: Scafetta, N. 2013. Discussion on climate oscillations: CMIP5 general circulation models versus a semi-empirical harmonic model based on astronomical cycles. Earth-Science Reviews 126, 321-357.

Luminosity production associated with the tidal energy dissipated in the Sun

$$\frac{L}{L_S} \approx \left(\frac{M}{M_S}\right)^4 \approx 1 + \frac{4\Delta M}{M_S},$$

rewriting it

$$L(t) \approx L_S + 4L_S \frac{\dot{U}_{tidal}(t)}{\dot{U}_{Sun}} = L_S + A \cdot \dot{U}_{tidal}(t),$$

A: amplification factor used in $K(\chi)$

$$\dot{U}_{Sun} = -\dot{U}_{fusion} = \frac{1}{2} G \int_0^{R_S} m_S(r) \frac{d\dot{m}(r)}{dr} \frac{1}{r} dr = 3.6 \times 10^{20} W,$$

$$\frac{d\dot{m}(r)}{dr} = \frac{1}{c^2} \frac{dL(r)}{dr},$$

$$A = \frac{4L_S}{\dot{U}_{Sun}} \approx 4.25 \times 10^6.$$

Equation to convert gravitational energy released by the tides into luminosity anomaly

$$I_P(t) = \frac{3GR_S^5}{2Q\Delta t} \int_0^1 K(\chi)\chi^4 \rho(\chi) d\chi.$$

$K(\chi)$ is the amplification function

$$\int_{\theta=0}^{\pi} \int_{\phi=0}^{2\pi} \left| \sum_{p=1}^{8} m_p \frac{\cos^2(\alpha_{p,t}) - \frac{1}{3}}{R_{sp}^3(t)} - m_p \frac{\cos^2(\alpha_{p,t-\Delta t}) - \frac{1}{3}}{R_{sp}^3(t-\Delta t)} \right| \sin(\theta)\, d\theta d\phi,$$

Solar luminosity $L_s = 4 \times 10^{26}$ W

Scafetta N., 2012. Does the Sun work as a nuclear fusion amplifier of planetary tidal forcing? A proposal for a physical mechanism based on the mass-luminosity relation. Journal of Atmospheric and Solar-Terrestrial Physics 81-82, 27-40.

The eccentricity variation of Jupiter versus the meteorite fall frequency (60-year)

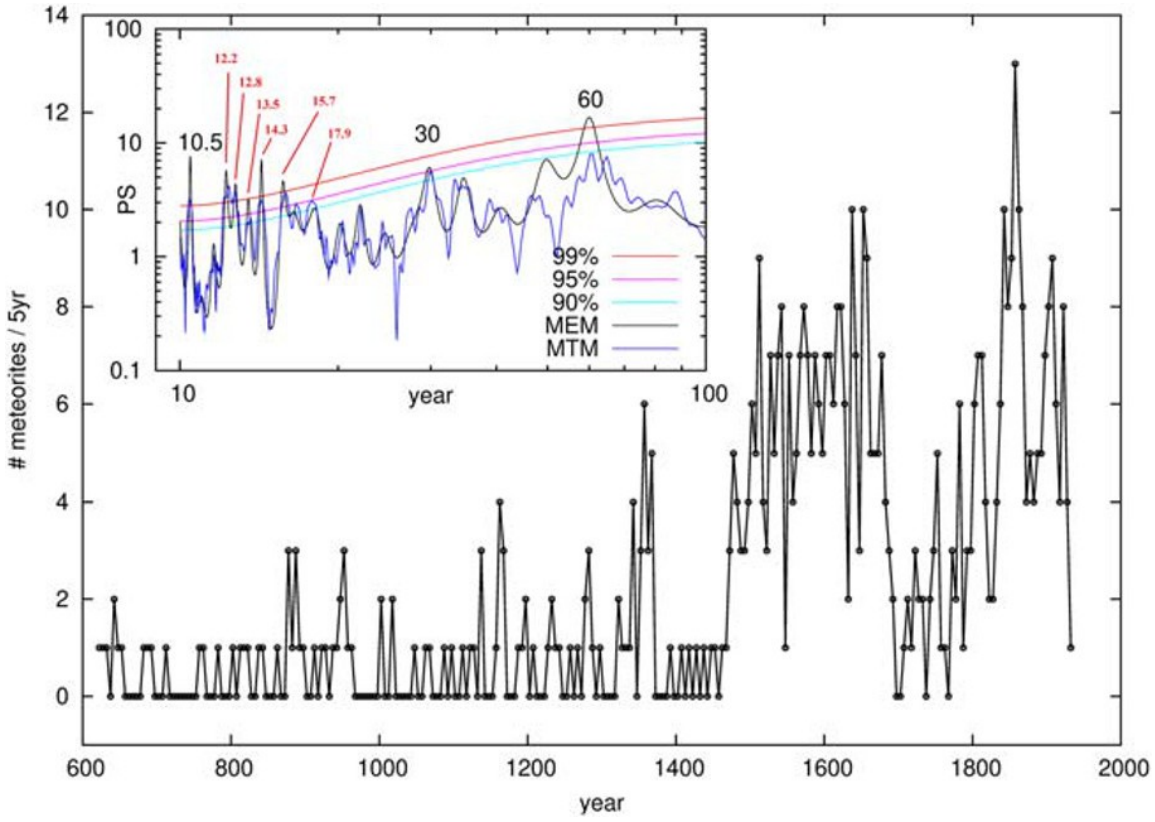

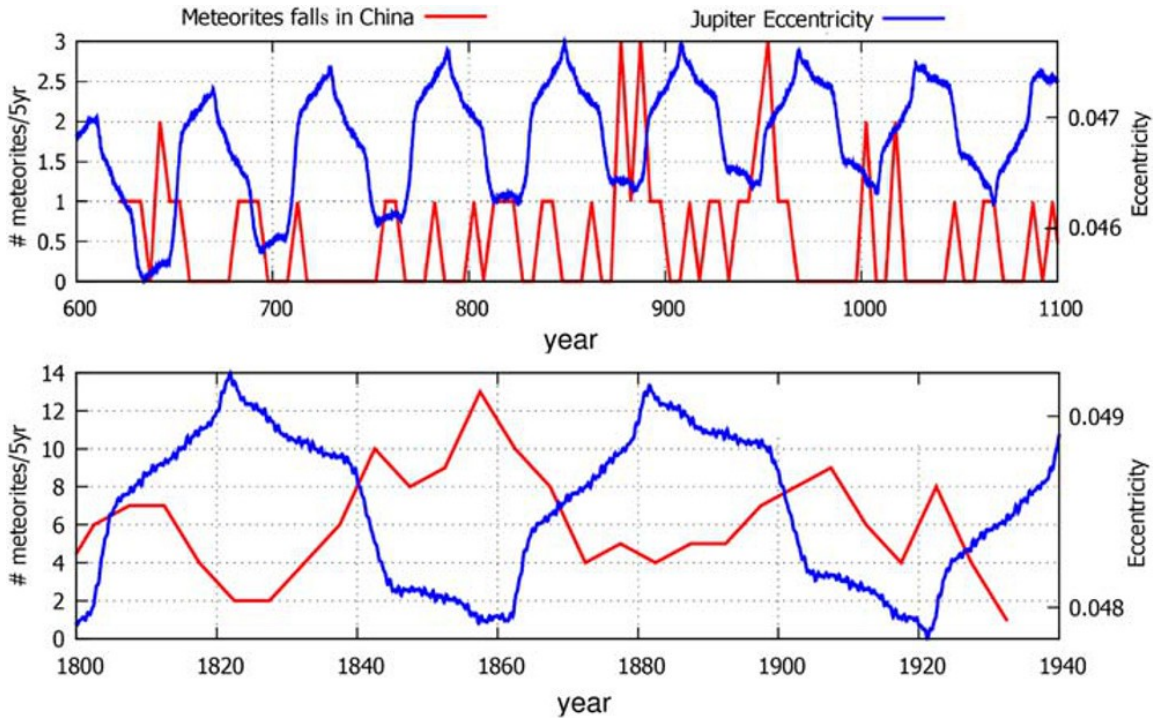

Scafetta, N., Milani, F., and Bianchini, A. (2020). A 60-Year Cycle in the Meteorite Fall Frequency Suggests a Possible Interplanetary Dust Forcing of the Earth's Climate Driven by Planetary Oscillations. Geophys. Res. Lett. 47 (18), e2020GL089954. doi:10.1029/2020gl089954

The harmonic organization of the solar system

- Bank MJ and Scafetta N (2022) Scaling, Mirror Symmetries and Musical Consonances Among the Distances of the Planets of the Solar System. Front. Astron. Space Sci. 8:758184. doi: 10.3389/fspas.2021.758184

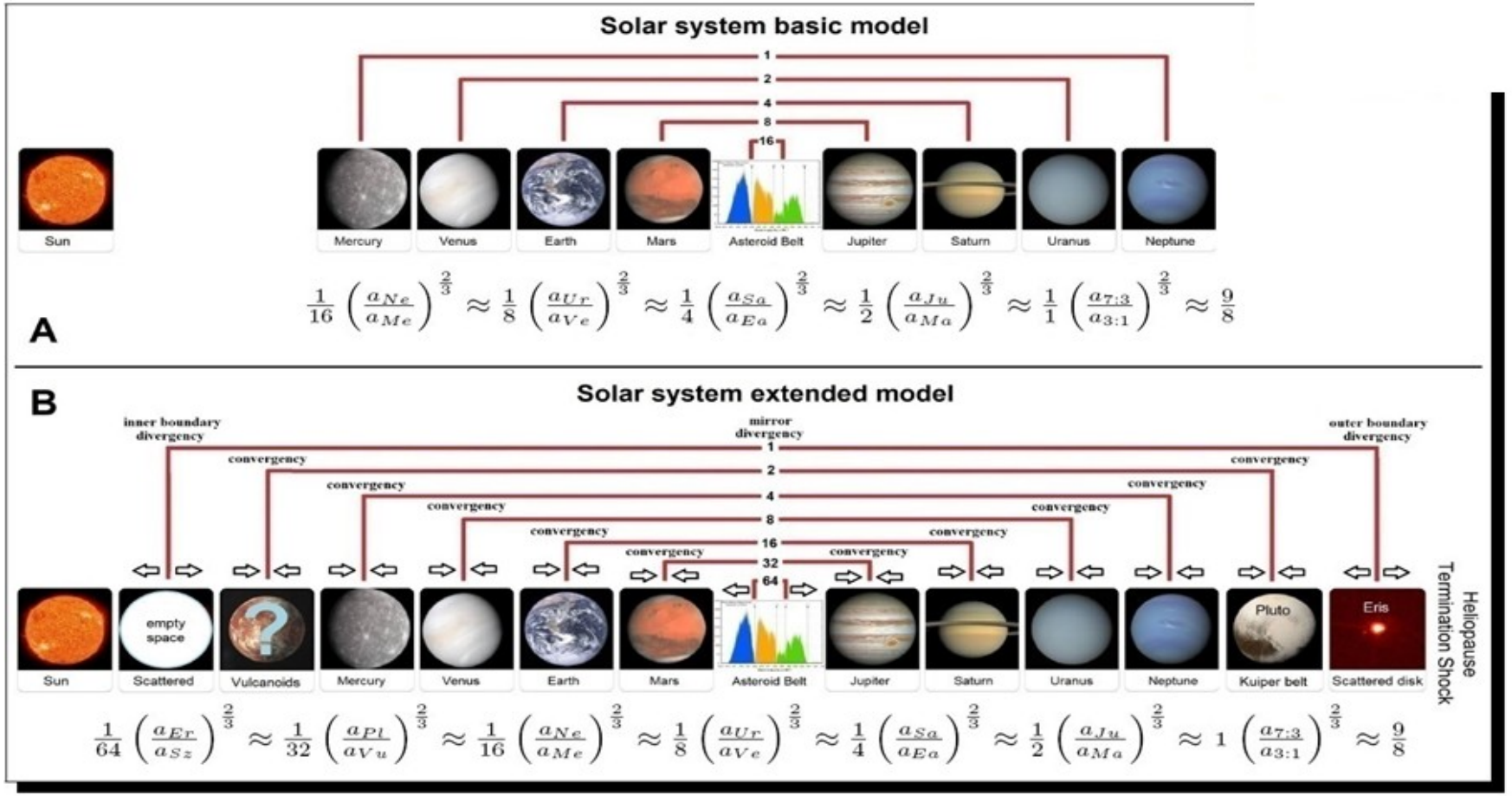

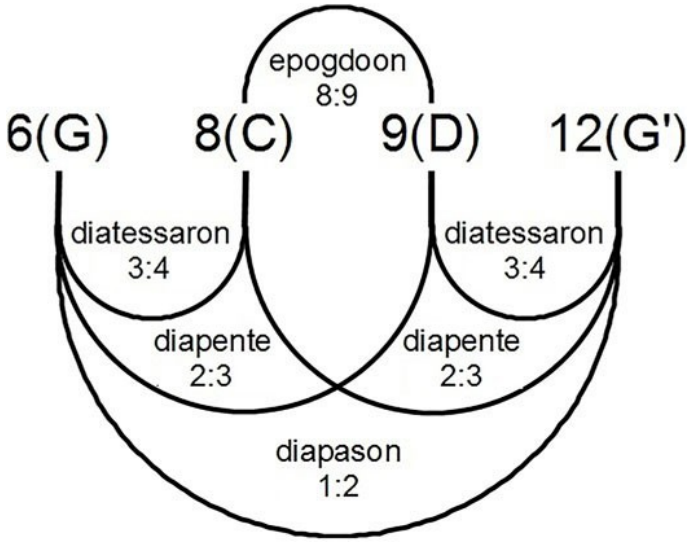

Pythagorean music theory

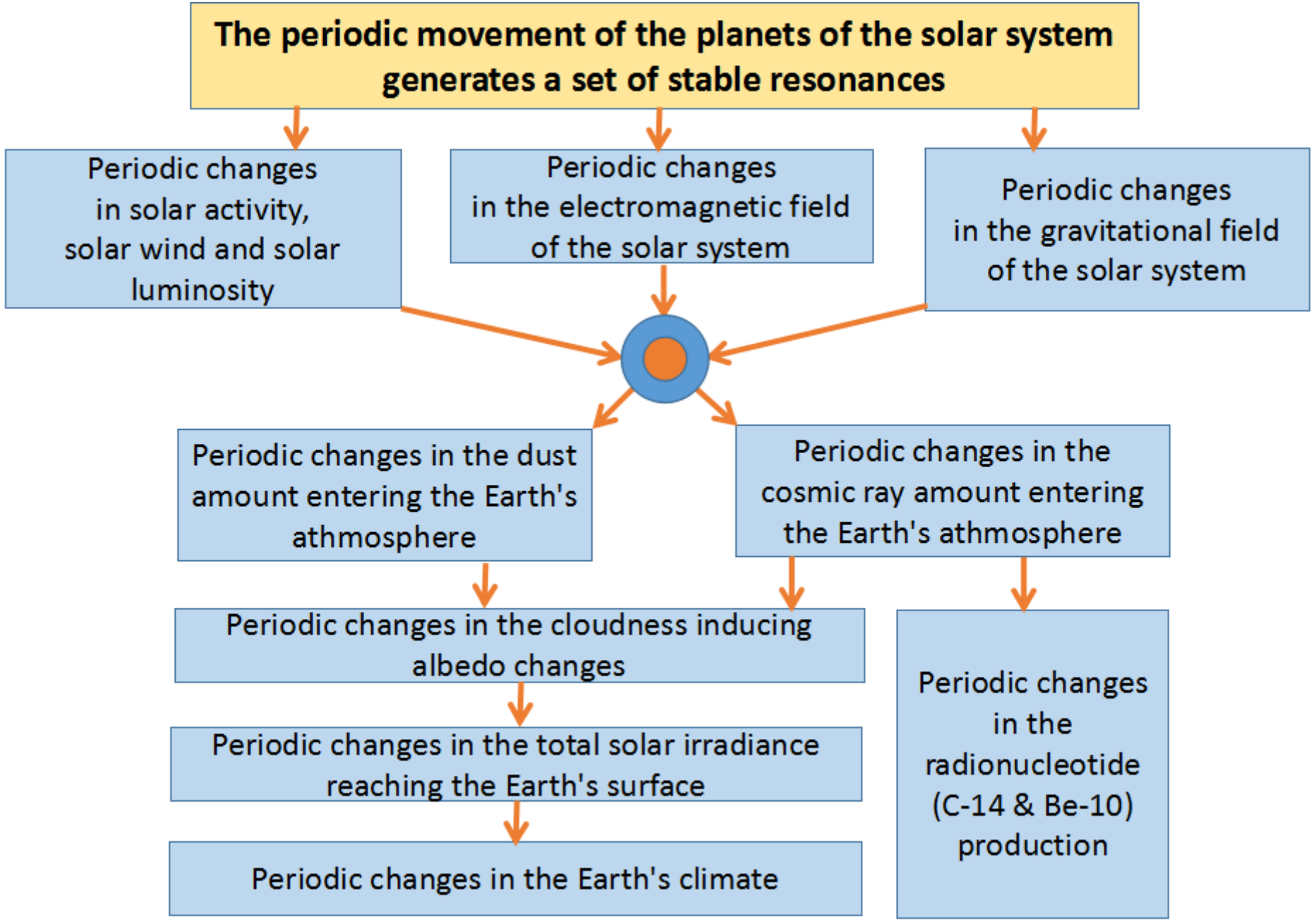
The periodic movement of the planets of the solar system generates a set of stable resonances
Periodic changes in solar activity, solar wind and solar luminosity
Periodic changes in the electromagnetic field of the solar system
Periodic changes in the gravitational field of the solar system
Periodic changes in the dust amount entering the Earth's athmosphere
Periodic changes in the cosmic ray amount entering the Earth's athmosphere
Periodic changes in the cloudness inducing albedo changes
Periodic changes in the total solar irradiance reaching the Earth's surface
Periodic changes in the Earth's climate
Periodic changes in the radionucleotide (C-14 & Be-10) production

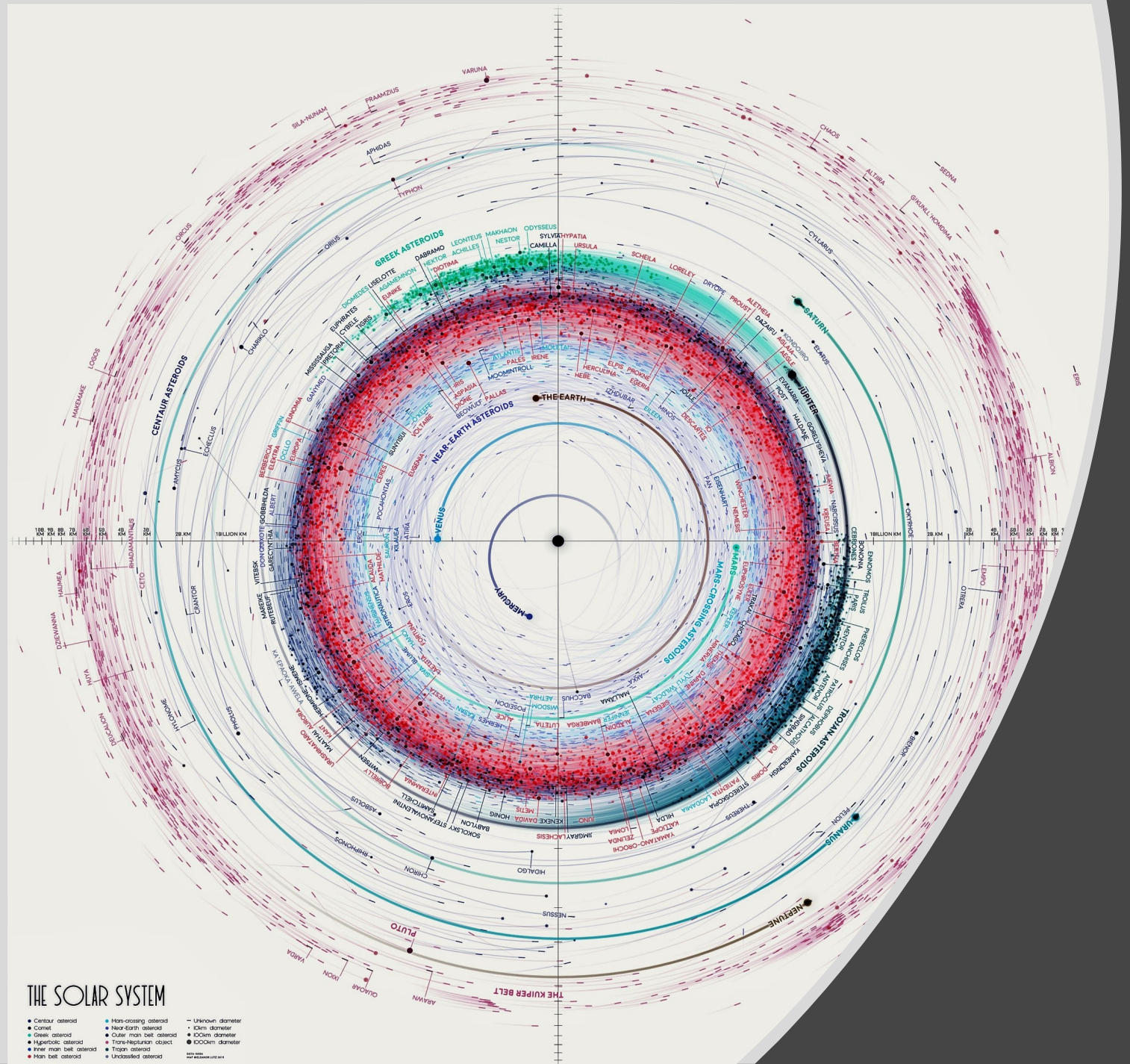

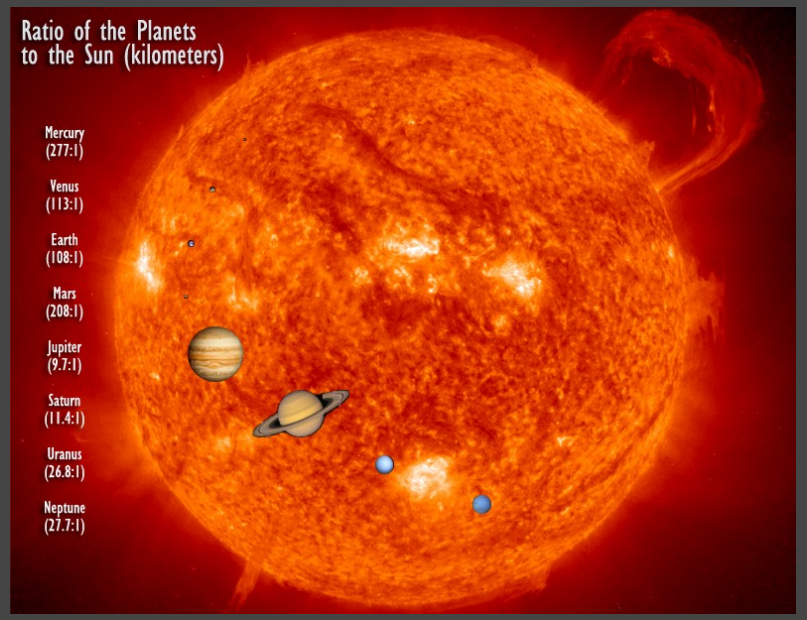

Conclusion

The solar system (including the Sun and the Earth) appears highly synchronized by the orbital motion of its planets.